



ELSEVIER

Available online at [www.sciencedirect.com](http://www.sciencedirect.com)

SCIENCE @ DIRECT®

Comput. Methods Appl. Mech. Engrg. 195 (2006) 65–93

**Computer methods  
in applied  
mechanics and  
engineering**

[www.elsevier.com/locate/cma](http://www.elsevier.com/locate/cma)

# Arbitrarily wide-angle wave equations for complex media

Murthy N. Guddati \*

*Department of Civil, Construction and Environmental Engineering, North Carolina State University,  
Campus Box 7908, Raleigh, NC 27695-7908, USA*

Received 24 May 2004; received in revised form 11 November 2004; accepted 11 January 2005

---

## Abstract

By combining various ideas related to one-way wave equations (OWWEs), half-space stiffness relation, special finite-element discretization, and complex coordinate stretching, a systematic procedure is developed for deriving a series of highly accurate space-domain versions of OWWEs. The resulting procedure is applicable to complex media where the governing equation (full wave equation) is a second order differential system, making the procedure applicable for general heterogeneous, anisotropic, porous, viscoelastic media. Owing to their high accuracy in representing waves propagating in an arbitrarily wide range of angles, the resulting equations are named Arbitrarily Wide-angle Wave Equations (AWWEs). In order to illustrate the proposed procedure, AWWEs are derived for one-way propagation in acoustic as well as elastic media. While acoustic AWWEs can be considered as modified versions of well-known space-domain OWWEs based on rational approximations of the square root operator, the elastic AWWEs are significantly different from the existing elastic OWWEs. Unlike the existing elastic OWWEs, elastic AWWEs are displacement-based and are applicable to general anisotropic media. Furthermore, AWWEs are simple in their form, and appear amenable to easy numerical implementation.

© 2005 Elsevier B.V. All rights reserved.

*Keywords:* One-way wave equations; Parabolic equations; Paraxial approximations; Seismic imaging; Synthetic aperture focusing technique (SAFT)

---

## 1. Introduction

Standard (full) wave equations are used to model the propagation of disturbances in acoustic and elastic media. These disturbances tend to propagate in all directions, i.e. in a  $360^\circ$  range. In contrast to full wave equations, one-way wave equations (OWWEs), as their name indicates, represent waves propagating in

---

\* Tel.: +1 919 515 7699; fax: +1 919 515 7908.

E-mail address: [mnguddat@ncsu.edu](mailto:mnguddat@ncsu.edu)

180° range of angles. Due to this special property, OWWEs are of interest in the areas such as (a) imaging in the contexts of geophysical migration (e.g. [1]) and nondestructive evaluation (NDE) (e.g. [2]), (b) range stepping in the context of underwater acoustics (e.g. [3]), and (c) absorbing boundaries in the contexts of unbounded domain modeling (e.g. [4,5]). In the special case of homogeneous media, exact OWWEs can be represented in frequency–wavenumber domain, and have been successfully used for imaging in acoustic as well as elastic media (e.g. phase-shift migration [6] and elasticity SAFT [7]). However, the frequency–wavenumber versions are not applicable for general heterogeneous media, where the equations should be written in frequency–space or time–space domains. Unfortunately, these versions contain complex pseudo-differential operators that require expensive computation. To alleviate the computational cost, OWWEs are often approximated, making their usage more practical. The resulting approximations can be either completely in space-domain, or in a dual-domain form (e.g. [8–10]). This paper focuses on approximate OWWEs that are completely in space-domain, i.e. time-space or frequency–space versions.

Approximations of acoustic OWWE in space domain have been developed and successfully used in various fields. Most of the developments are based on rational approximation of the square-root operator occurring in the dispersion relationship of the exact OWWE. Claerbout [1] used low order rational approximations to develop the so-called 15° and 45° wave equations that are widely used for geophysical imaging. Lindman [11] and Engquist and Majda [4] used higher order approximations to develop absorbing boundary conditions for modeling homogeneous unbounded domains. Later, these ideas were continuously refined by various researchers; one of the noteworthy contributions is by Bamberger et al. [12,13], who developed higher order approximations of OWWE extendable to heterogeneous media. These OWWEs are successfully implemented by Collins [14] for range-stepping in the contexts of ocean acoustics. Similar OWWEs were developed and utilized in the contexts of unbounded domain modeling (see [15] for a survey).

Development of time–space and frequency–space OWWEs for elastic media have been largely limited to range-stepping problems. Early developments of Elastic OWWEs were by Landers and Claerbout [16], McCoy [17], Wales and McCoy [18], Hudson [19], Corones et al. [20], and Greene [21], which were later enhanced by Wetton and Brooke [22], Collins [23], and Fredericks et al. [24]. With the exception of Hudson's formulation, which is only first order accurate, the existing elastic OWWEs are in terms of displacement potentials, displacements and dilatations, or displacements and derivatives. While these formulations may be converted in terms of displacements, such converted formulations tend to be complex and are not readily amenable for implementation, especially in the contexts of imaging and unbounded domain analysis. More importantly, existing elastic OWWEs are limited to either isotropic or transversely isotropic elastic media with a principal material direction coinciding with the one-way propagation direction [24]. However, in many situations, this may not be the case, e.g. in the context of geophysical imaging, tectonic forces may change the direction of bedding causing the principal material direction not coinciding with the desired (vertical) direction of one-way propagation. It is desirable to obtain *displacement-based* OWWEs that are applicable for *general anisotropic elastic materials*.

In order to model wave propagation in soils and other geological materials such as ocean-bottom sediments and hydrocarbon reservoirs, it would be useful to obtain OWWEs that consider the multi-phase (solid and fluids) poroelastic deformation. Although poroelastic OWWEs have been successfully developed [25], the current versions are based on the ideas related to existing elastic OWWEs, and have the same limitations as elastic OWWEs. It is thus desirable to obtain displacement-based OWWEs that can accurately simulate one-way propagation in elastic as well as poroelastic media.

With the ultimate goal of developing time–space and frequency–space OWWEs for anisotropic poroelastic media directly in terms of displacements, we develop in this paper a new framework for the systematic derivation of highly accurate approximations of OWWEs for complex elastic media. The proposed framework is based on a series of ideas that eventually relate OWWEs to special finite-element discretization of

the half-space stiffness relations. The procedure is applicable for complex media including anisotropic, viscous and porous elastic media, but is limited to range-independent problems (i.e., the material properties do not vary in the principal propagation direction). OWWEs resulting from this derivation procedure can be made accurate for arbitrarily wide range of propagation angles and hence named Arbitrarily Wide-Angle Wave Equations (AWWEs). In addition to propagating waves, AWWEs have the flexibility to represent evanescent waves, which are sometimes needed for stable implementation [26]. In spite of their high accuracy, AWWEs take the simple form of the well-known 15° equation of geophysical prospecting (or the basic parabolic equation in the context of underwater acoustics). In addition to the AWWE derivation procedure and the proof of its validity, this paper contains illustration of the AWWE's accuracy for acoustic, isotropic elastic and some special cases of anisotropic elastic media.

The outline of the paper is as follows. Section 2 contains a brief review of various wave equations ranging from the acoustic wave equation to the more complex anisotropic poroelastic wave equation. This section concludes with two model equations, one representing simple acoustic waves, and the other representing waves in viscoelastic porous media. In Section 3, the ideas of OWWEs are presented, with some overview of classical techniques and the difficulties associated with deriving OWWEs for complex media. Section 4 contains the idea of obtaining OWWE using the half-space stiffness relation, eventually resulting in a recursive variational definition of the exact OWWE. In Section 5, the resulting variational definition is discretized using a special finite-element scheme, leading to discrete but exact definition OWWE containing an infinite number of auxiliary variables. The arbitrarily wide-angle wave equations (AWWEs) are derived in their final form in Section 6 by (a) approximating the exact OWWE by limiting the number auxiliary variables and (b) choosing special discretization parameters. In Section 7, the resulting general form of AWWE is specialized for acoustic as well as elastic media, and their accuracy is examined for isotropic as well as anisotropic media. The paper concludes with some closing remarks in Section 8.

## 2. Preliminaries: wave propagation in complex media

This section contains a summary of various types of wave equations governing propagation of disturbances in media ranging from isotropic acoustic media to anisotropic poroelastic media. The discussion is limited to propagation of small disturbances, i.e. geometric and material nonlinearities are not considered, resulting in linear wave equations. Many equations are not derived here, but borrowed from standard references. The equations are written in Cartesian coordinate system to facilitate easy presentation. Furthermore, they are written for two spatial dimensions, but the method presented in this paper is easily extendable to three-dimensional systems.

### 2.1. Acoustic waves

Propagation of disturbances in inviscid fluids can be represented by the acoustic wave equation given by [27]

$$\frac{1}{\lambda} \frac{\partial^2 \psi(x, z; t)}{\partial t^2} - \nabla \cdot \left( \frac{1}{\rho} \nabla \psi(x, z; t) \right) = 0, \quad (1)$$

where  $\psi(x, z; t)$  is the field variable (acoustic pressure),  $\lambda$  is the bulk modulus, and  $\rho$  is the density. Although the above equation is valid for wave propagation in fluids, the equation has been used for pressure wave propagation in solids. Because of its simplicity, the above equation has been the most widely used equation, with significant work done in the context of one-way wave equations.

## 2.2. Elastic waves

Wave propagation in elastic media is more complicated than acoustic waves because of the complex coupling between pressure and shear waves [28]. Adding to this complexity, sometimes the material is not isotropic, indicating that the wave velocities vary depending on the direction of propagation. There may be some axes of material symmetry (e.g. transversely isotropic media often encountered in geological materials), but they may not always coincide with the coordinate system under consideration (e.g. dipping bedding due to tectonic forces). It is thus instructive to consider the general elastic wave equation in non-homogeneous anisotropic elastic solid. Such an equation is derived from (a) equations of motion or dynamic equilibrium given by

$$\begin{bmatrix} \partial/\partial x & 0 \\ 0 & \partial/\partial z \\ \partial/\partial z & \partial/\partial x \end{bmatrix}^T \boldsymbol{\sigma} = \rho \frac{\partial^2 \mathbf{u}}{\partial t^2}, \quad (2)$$

(b) stress–strain relations:

$$\boldsymbol{\sigma} = \begin{bmatrix} E_{11} & E_{12} & E_{13} \\ E_{12} & E_{22} & E_{23} \\ E_{13} & E_{23} & E_{33} \end{bmatrix} \boldsymbol{\varepsilon}, \quad (3)$$

and (c) linear strain–displacement relations:

$$\boldsymbol{\varepsilon} = \begin{bmatrix} \partial/\partial x & 0 \\ 0 & \partial/\partial z \\ \partial/\partial z & \partial/\partial x \end{bmatrix} \mathbf{u}. \quad (4)$$

In the above  $\mathbf{u} = \{u_x \ u_z\}^T$  is the displacement vector,  $\boldsymbol{\sigma} = \{\sigma_{xx} \ \sigma_{zz} \ \tau_{xz}\}^T$  is the stress tensor written in vector form,  $\boldsymbol{\varepsilon} = \{\varepsilon_{xx} \ \varepsilon_{zz} \ \gamma_{xz}\}^T$  is the infinitesimal strain vector. Combining (2)–(4), the general elastic wave equation in heterogeneous anisotropic elastic media can be written as

$$\frac{\partial}{\partial x} \left( \mathbf{G}_{xx} \frac{\partial \mathbf{u}}{\partial x} \right) + \frac{\partial}{\partial x} \left( \mathbf{G}_{xz} \frac{\partial \mathbf{u}}{\partial z} \right) + \frac{\partial}{\partial z} \left( \mathbf{G}_{xz}^T \frac{\partial \mathbf{u}}{\partial x} \right) + \frac{\partial}{\partial z} \left( \mathbf{G}_{zz} \frac{\partial \mathbf{u}}{\partial z} \right) = \mathbf{M} \frac{\partial^2 \mathbf{u}}{\partial t^2}, \quad (5)$$

where the coefficient matrices represent stiffness and inertial resistance properties and are given by

$$\mathbf{G}_{xx} = \begin{bmatrix} E_{11} & E_{13} \\ E_{13} & E_{33} \end{bmatrix}, \quad \mathbf{G}_{xz} = \begin{bmatrix} E_{13} & E_{12} \\ E_{33} & E_{23} \end{bmatrix}, \quad \mathbf{G}_{zz} = \begin{bmatrix} E_{33} & E_{23} \\ E_{23} & E_{22} \end{bmatrix}, \quad \mathbf{M} = \begin{bmatrix} \rho & 0 \\ 0 & \rho \end{bmatrix}. \quad (6)$$

A special case of interest is isotropic elasticity, where the material coefficients are given in terms of Lamé moduli,  $\lambda$  and  $\mu$ :

$$E_{11} = E_{22} = \lambda + 2\mu, \quad E_{12} = \lambda, \quad E_{13} = E_{23} = 0, \quad E_{33} = \mu. \quad (7)$$

Anti-plane shear wave propagation in anisotropic solids takes a form similar to (5), except that the field variable  $\mathbf{u}$  is replaced by the scalar anti-plane displacement  $u = u_y$ , and the coefficient matrices will simply be scalars. For the special case of isotropy, the equation takes the simpler form:

$$\frac{\partial}{\partial x} \left( \mu \frac{\partial u}{\partial x} \right) + \frac{\partial}{\partial z} \left( \mu \frac{\partial u}{\partial z} \right) = \rho \frac{\partial^2 u}{\partial t^2}, \quad (8)$$

which is similar to the acoustic wave equation (1).

### 2.3. Waves in more complex media

Many materials such as soils, ocean-bottom sediments, and biological materials are more complex than elastic materials in that there are effects of pore fluid and the solid skeleton itself could have time-dependent behavior. The time-dependent characteristic is often modeled through viscoelasticity. The wave equation for linear viscoelastic materials is modeled using an equation similar to the elastic wave equation, with the difference being the material matrices  $\mathbf{G}_{xx}$ ,  $\mathbf{G}_{xz}$ ,  $\mathbf{G}_{zz}$  are now differential/integral operators in time.

Wave propagation in poroelastic media is significantly more complex than elastic media in that the complex deformation of solid skeleton is further coupled with the flow of the pore fluid. As an example, we write here the wave equation in anisotropic saturated poroelastic media (extended from Eq. (6.7) in [29]):

$$\frac{\partial}{\partial x} \left( \mathbf{G}_{xx} \frac{\partial \mathbf{u}}{\partial x} \right) + \frac{\partial}{\partial x} \left( \mathbf{G}_{xz} \frac{\partial \mathbf{u}}{\partial z} \right) + \frac{\partial}{\partial z} \left( \mathbf{G}_{xz}^T \frac{\partial \mathbf{u}}{\partial x} \right) + \frac{\partial}{\partial z} \left( \mathbf{G}_{zz} \frac{\partial \mathbf{u}}{\partial z} \right) = \mathbf{M} \frac{\partial^2 \mathbf{u}}{\partial t^2} + \mathbf{C} \frac{\partial \mathbf{u}}{\partial t}. \quad (9)$$

In the above, the field variable contains not only the displacement vector of the solid phase, but also that of the fluid phase:

$$\mathbf{u} = \{ u_x^s \quad u_z^s \quad u_x^f \quad u_z^f \}^T. \quad (10)$$

The stiffness related coefficient matrices are given by

$$\mathbf{G}_{xx} = \begin{bmatrix} E_{11} & E_{13} & Q & 0 \\ E_{13} & E_{33} & 0 & 0 \\ Q & 0 & R & 0 \\ 0 & 0 & 0 & 0 \end{bmatrix}, \quad \mathbf{G}_{xz} = \begin{bmatrix} E_{13} & E_{12} & 0 & Q \\ E_{33} & E_{23} & 0 & 0 \\ 0 & Q & R & 0 \\ 0 & 0 & 0 & R \end{bmatrix}, \quad \mathbf{G}_{zz} = \begin{bmatrix} E_{33} & E_{23} & 0 & 0 \\ E_{23} & E_{22} & 0 & Q \\ 0 & 0 & 0 & 0 \\ 0 & Q & 0 & R \end{bmatrix}, \quad (11)$$

where  $Q$  represents the coupling stiffness and  $R$  is related to the bulk modulus of the fluid. The matrix associated with inertial effects is given by

$$\mathbf{M} = \begin{bmatrix} \rho_s + \rho_a & 0 & -\rho_a & 0 \\ 0 & \rho_s + \rho_a & 0 & -\rho_a \\ -\rho_a & 0 & \rho_f + \rho_a & 0 \\ 0 & -\rho_a & 0 & \rho_f + \rho_a \end{bmatrix}. \quad (12)$$

In the above,  $\rho_s$  and  $\rho_f$  are average densities of solid and fluid phases respectively, while  $\rho_a$  is the added mass term. The matrix  $\mathbf{C}$  is associated with the damping due to viscous flow of pore fluid and is given by

$$\mathbf{C} = \frac{\eta \beta^2}{\kappa} \begin{bmatrix} 1 & 0 & -1 & 0 \\ 0 & 1 & 0 & -1 \\ -1 & 0 & 1 & 0 \\ 0 & -1 & 0 & 1 \end{bmatrix}, \quad (13)$$

where  $\eta$  is the pore-fluid viscosity,  $\beta$  is the porosity, and  $\kappa$  is the Darcy permeability.

### 2.4. Model equations

To facilitate easy presentation of the proposed procedure, we consider two model equations representing the two extremes of complexity. The first is the *scalar wave equation*

$$\frac{\partial}{\partial x} \left( \mu \frac{\partial u}{\partial x} \right) + \frac{\partial}{\partial z} \left( \mu \frac{\partial u}{\partial z} \right) - \rho \frac{\partial^2 u}{\partial t^2} = 0, \quad (14)$$

representing acoustic waves (1) and anti-plane shear waves in isotropic media (8). The second model equation is the most complex wave equation discussed above, namely the wave equation for viscoelastic porous media:

$$\frac{\partial}{\partial x} \left( \mathbf{G}_{xx} \frac{\partial \mathbf{u}}{\partial x} \right) + \frac{\partial}{\partial x} \left( \mathbf{G}_{xz} \frac{\partial \mathbf{u}}{\partial z} \right) + \frac{\partial}{\partial z} \left( \mathbf{G}_{xz}^T \frac{\partial \mathbf{u}}{\partial x} \right) + \frac{\partial}{\partial z} \left( \mathbf{G}_{zz} \frac{\partial \mathbf{u}}{\partial z} \right) - \mathbf{M} \frac{\partial^2 \mathbf{u}}{\partial t^2} - \mathbf{C} \frac{\partial \mathbf{u}}{\partial t} = \mathbf{0}, \quad (15)$$

where  $\mathbf{G}_{xx}$ ,  $\mathbf{G}_{xz}$ ,  $\mathbf{G}_{zx}$ ,  $\mathbf{G}_{zz}$  are operators with time derivatives, representing viscoelastic behavior of the material. In this paper, we refer to the above equation as the *vector wave equation*.

For most of the paper, we will focus on frequency domain equations, noting that the final equations can be easily transformed back to time domain. The notation used for field variables and coefficient matrices are the same in the frequency and time domains, but it should be noted that in frequency domain, they refer to transformed variables and operators. Furthermore, time-harmonic motion is chosen to be of the form  $e^{-i\omega t}$ . The scalar wave equation then transforms into

$$\frac{\partial}{\partial x} \left( \mu \frac{\partial u}{\partial x} \right) + \frac{\partial}{\partial z} \left( \mu \frac{\partial u}{\partial z} \right) + \rho \omega^2 u = 0. \quad (16)$$

The vector wave equation is given by

$$\frac{\partial}{\partial x} \left( \mathbf{G}_{xx} \frac{\partial \mathbf{u}}{\partial x} \right) + \frac{\partial}{\partial x} \left( \mathbf{G}_{xz} \frac{\partial \mathbf{u}}{\partial z} \right) + \frac{\partial}{\partial z} \left( \mathbf{G}_{xz}^T \frac{\partial \mathbf{u}}{\partial x} \right) + \frac{\partial}{\partial z} \left( \mathbf{G}_{zz} \frac{\partial \mathbf{u}}{\partial z} \right) + (\omega^2 \mathbf{M} + i\omega \mathbf{C}) \mathbf{u} = \mathbf{0}, \quad (17)$$

where the stiffness related coefficient matrices  $\mathbf{G}_{xx}$ ,  $\mathbf{G}_{xz}$ ,  $\mathbf{G}_{zz}$  are functions of  $\omega$ .

### 3. One-way wave equations (OWWEs)

It is well known that Eqs. (16) and (17) admit waves propagating in all directions, i.e. in a  $360^\circ$  range. The goal of the paper is to obtain one-way wave equations (OWWEs) that propagate waves only in a  $180^\circ$  range. Without any loss of generality, we focus our presentation on OWWEs representing waves propagating in the positive  $x$  direction. To this end, we start by writing the model wave equations as linear differential equations in  $x$ . From this point onwards, we limit our development to range-independent media, i.e., the material properties do not vary with  $x$ . The scalar wave equation is written as

$$\frac{\partial}{\partial x} \left( A(z; \omega) \frac{\partial u}{\partial x} \right) + D(z; \omega) u = 0, \quad (18)$$

where  $A$  and  $D$  are *scalar* differential operators in  $z$ . Similarly, the vector wave equation is written as

$$\frac{\partial}{\partial x} \left( \mathbf{A}(z; \omega) \frac{\partial \mathbf{u}}{\partial x} \right) + \frac{\partial}{\partial x} (\mathbf{B}_1(z; \omega) \mathbf{u}) + \mathbf{B}_2(z; \omega) \frac{\partial \mathbf{u}}{\partial x} + \mathbf{D}(z; \omega) \mathbf{u} = \mathbf{0}, \quad (19)$$

where  $\mathbf{A}$ ,  $\mathbf{B}_1$ ,  $\mathbf{B}_2$ ,  $\mathbf{D}$  are *matrix* differential operators in  $z$ . Focusing on the more general vector wave equation, the general form of the solution is given by

$$\mathbf{u}(x, z; \omega) = \mathbf{a}(z; \omega) e^{ikx}, \quad (20)$$

where  $k$  is the (horizontal) wavenumber. The wavenumber can be obtained by substituting (20) in (19):

$$[-k^2 \mathbf{A} + ik(\mathbf{B}_1 + \mathbf{B}_2) + \mathbf{D}] \mathbf{a} = \mathbf{0}. \quad (21)$$

Essentially  $k$  would be the roots of the dispersion relation:

$$\text{Det}[-k^2 \mathbf{A} + ik(\mathbf{B}_1 + \mathbf{B}_2) + \mathbf{D}] = 0. \quad (22)$$

It is easy to see that the dispersion relation contains  $m$  pairs of complex conjugate roots. The wavenumbers with positive real part would represent waves propagating in the positive  $x$  direction, while a negative real part would indicate that waves are propagating in the negative  $x$  direction. The desired OWWE can thus be considered as a factor of full wave equations that contains only the roots with non-negative real parts. Effectively, OWWE can be written as

$$\frac{\partial \mathbf{u}}{\partial x} = \mathbf{i}\Lambda \mathbf{u}, \quad (23)$$

where  $\Lambda$  is a matrix operator with its eigenvalues coinciding with the wavenumbers with non-negative real parts. The main task in deriving OWWE is to obtain the operator  $\Lambda$ .

Formal representation of OWWE operator ( $\Lambda$ ) is straightforward in the context of scalar wave equation (18), which can be formally factorized as

$$\left( \frac{\partial}{\partial x} - i\sqrt{\frac{D}{A}} \right) \left( \frac{\partial}{\partial x} + i\sqrt{\frac{D}{A}} \right) u = 0, \quad (24)$$

where  $\sqrt{D/A}$  represents the positive square root, containing only the positive eigenvalues of  $D$  with respect to  $A$ . It immediately follows that the first factor represents forward propagating waves while the second factor represents backward propagating waves. Thus the desired OWWE, representing waves propagating in the positive  $x$  direction, can be formally written a

$$\frac{\partial u}{\partial x} = i\sqrt{\frac{D}{A}}u, \quad (25)$$

indicating that  $\Lambda = \sqrt{D/A}$  for the scalar case. The above form of OWWE is deceptively simple; the formal square root results in pseudo-differential operator, which is an expensive convolution operator in the spatial ( $z$ ) domain. In order to obtain a more tractable OWWE, rational approximation of the square-root operator is used to approximate the pseudo-differential form (25) into a differential form. There has been significant success in the development and implementation of differential versions of acoustic OWWE, with more accurate approximations representing one-way propagation in almost  $180^\circ$  range [12].

Obtaining differential OWWEs for more complex waves have not been equally successful. The difficulty stems from the fact that (19) cannot be directly factorized the way (18) has been factorized into (24). Modifying the wave equations in terms of dilatation and displacement ( $\nabla \cdot \mathbf{u}$ ,  $u_z$ ) or displacement derivative and displacement ( $\partial u_x / \partial x$ ,  $u_z$ ) would facilitate factorization, but only for some special cases such as transversely isotropic elasticity with an axis of material symmetry aligned with the  $x$  axis. Furthermore, in the context of imaging, the dilatation or the derivative of the displacement are not known at the surface for the purposes of downward continuation. While the existing formulations can be converted in terms of displacements, such conversions tend to be not amenable for numerical implementation. It is thus desirable to obtain a factorization procedure that works directly in terms of displacements and is applicable to more general cases of anisotropic elastic and poroelastic media.

This paper presents a novel procedure to systematically develop approximate OWWEs starting from the general full wave equation of the form (19) and is formulated directly in terms of the displacement. The resulting approximations are called arbitrarily wide-angle wave equations (AWWEs) as they can be accurate up to  $\pm 90^\circ$ . These equations are derived based on the relationship between OWWE and half-space stiffness, and take a form similar to the continued-fraction-based acoustic OWWE derived in the context of absorbing boundary conditions [5].

#### 4. Variational form of OWWE from half-space stiffness relations

Consider a half-space ( $x_0 < x < \infty$ ) excited at the left boundary  $x = x_0$ . The dynamic stiffness  $\mathbf{K}$  (also called the Dirichlet-to-Neumann map) of the half-space, by definition, relates the displacement  $\mathbf{u}_0$  at the left boundary to the traction  $\mathbf{F}_0$  at the boundary:

$$\mathbf{F}_0 = \mathbf{K}\mathbf{u}_0. \quad (26)$$

We consider two ways of evaluating the stiffness operator  $\mathbf{K}$ . In the *first approach*, the half-space is split into a layer ( $\Omega_1 \equiv \{x_0 < x < x_1\}$ ) and another half-space ( $x > x_1$ ), as shown in Fig. 1b. The governing equation is satisfied in the layer ((19) is rewritten here):

$$\frac{\partial}{\partial x} \left( \mathbf{A} \frac{\partial \mathbf{u}}{\partial x} \right) + \frac{\partial}{\partial x} (\mathbf{B}_1 \mathbf{u}) + \mathbf{B}_2 \frac{\partial \mathbf{u}}{\partial x} + \mathbf{D}\mathbf{u} = \mathbf{0} \quad \text{for } x_0 < x < x_1. \quad (19)$$

The boundary conditions on the left and right edges of the layer are

$$\begin{aligned} \mathbf{F}_0 &= - \left( \mathbf{A} \frac{\partial \mathbf{u}}{\partial x} + \mathbf{B}_1 \mathbf{u} \right) \Big|_{x=x_0} = \mathbf{K}\mathbf{u}_0, \\ \mathbf{F}_1 &= - \left( \mathbf{A} \frac{\partial \mathbf{u}}{\partial x} + \mathbf{B}_1 \mathbf{u} \right) \Big|_{x=x_1} = \mathbf{K}\mathbf{u}_1. \end{aligned} \quad (27)$$

Eq. (19) can be written in variational form:

$$\int_{x=x_0}^{x=x_1} \delta \mathbf{u}^T \left[ \frac{\partial}{\partial x} \left( \mathbf{A} \frac{\partial \mathbf{u}}{\partial x} \right) + \frac{\partial}{\partial x} (\mathbf{B}_1 \mathbf{u}) + \mathbf{B}_2 \frac{\partial \mathbf{u}}{\partial x} + \mathbf{D}\mathbf{u} \right] dx = 0 \quad \text{for all } \delta \mathbf{u}. \quad (28)$$

Using integration by parts for the first two terms in the integrand, we obtain

$$\left[ -\delta \mathbf{u}^T \left( \mathbf{A} \frac{\partial \mathbf{u}}{\partial x} + \mathbf{B}_1 \mathbf{u} \right) \right]_{x=x_0}^{x=x_1} + \int_{x=x_0}^{x=x_1} \left[ -\frac{\partial \delta \mathbf{u}^T}{\partial x} \mathbf{A} \frac{\partial \mathbf{u}}{\partial x} - \frac{\partial \delta \mathbf{u}^T}{\partial x} \mathbf{B}_1 \mathbf{u} + \delta \mathbf{u}^T \mathbf{B}_2 \frac{\partial \mathbf{u}}{\partial x} + \delta \mathbf{u}^T \mathbf{D}\mathbf{u} \right] dx = 0. \quad (29)$$

Substituting the boundary conditions (27) in (29), we obtain a recursive variational definition of the half-space stiffness:

$$\delta \mathbf{u}_0^T \mathbf{K}\mathbf{u}_0 = \delta \mathbf{u}_1^T \mathbf{K}\mathbf{u}_1 + \int_{x=x_0}^{x=x_1} \left[ \frac{\partial \delta \mathbf{u}^T}{\partial x} \mathbf{A} \frac{\partial \mathbf{u}}{\partial x} + \frac{\partial \delta \mathbf{u}^T}{\partial x} \mathbf{B}_1 \mathbf{u} - \delta \mathbf{u}^T \mathbf{B}_2 \frac{\partial \mathbf{u}}{\partial x} - \delta \mathbf{u}^T \mathbf{D}\mathbf{u} \right] dx. \quad (30)$$

The *second way* of obtaining half-space stiffness is by using OWWE. Noting that waves in the half-space (excited at the boundary) travel only in the positive  $x$  direction, the displacement in the half-space satisfies OWWE, which is of the form given in (23). It follows that the traction can be obtained in a straightforward manner:

$$\mathbf{F}_0 = - \left( \mathbf{A} \frac{\partial \mathbf{u}}{\partial x} + \mathbf{B}_1 \mathbf{u} \right) \Big|_{x=x_0} = -(\mathbf{iA}\boldsymbol{\Lambda} + \mathbf{B}_1)\mathbf{u}_0, \quad (31)$$

indicating that the stiffness is given by

$$\mathbf{K} = -(\mathbf{iA}\boldsymbol{\Lambda} + \mathbf{B}_1) \quad (32)$$

in other words, the OWWE in (23) can be rewritten as

$$\mathbf{A} \frac{\partial \mathbf{u}}{\partial x} + (\mathbf{B}_1 + \mathbf{K})\mathbf{u} = \mathbf{0}, \quad (33)$$

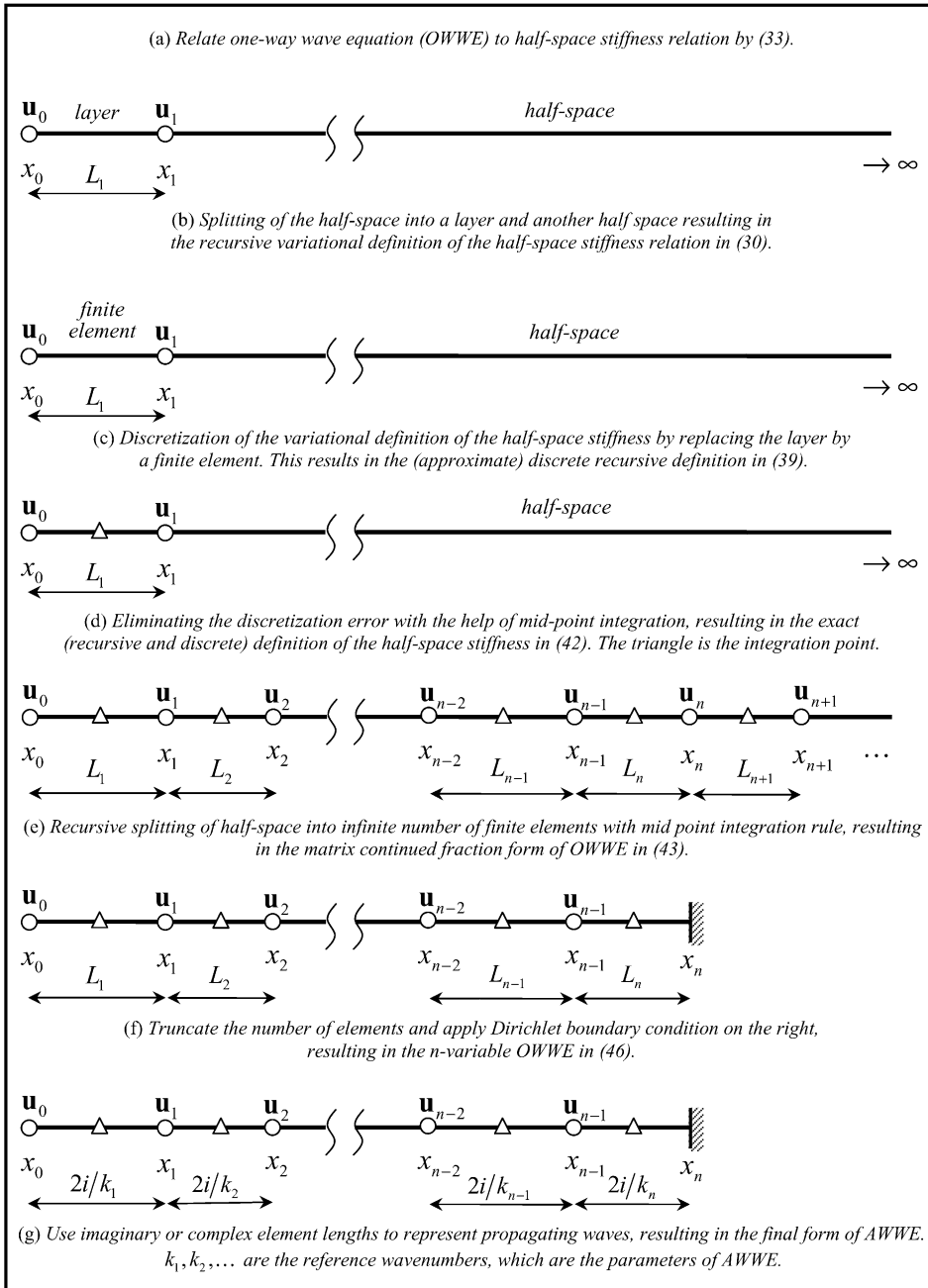


Fig. 1. Steps in the derivation of Arbitrarily Wide-Angle Wave Equations (AWWEs).

where  $\mathbf{K}$  is defined by (30). Because of the variational form of the definition of  $\mathbf{K}$ , we call the above equation the *variational OWWE*. Note that this is an exact equation with *no approximations* made so far.

### 5. Continued-fraction expansion of OWWE through finite-element discretization

The variational OWWE defined by (33) and (30) is just as intractable as the pseudo-differential form of OWWE given by (23). In this section, we work towards obtaining a more tractable OWWE. To this end, the half-space stiffness relation in (30) is discretized using Galerkin finite element method. Albeit potentially inaccurate, the simplest discretization is to replace the layer  $\Omega_1$  with a single finite element with two nodes at  $x_0$  and  $x_1$ , with the displacement varying linearly between the two nodes (Fig. 1c):

$$\mathbf{u} \approx \mathbf{N}_1 \begin{Bmatrix} \mathbf{u}_0 \\ \mathbf{u}_1 \end{Bmatrix} \quad \text{in } \Omega_1. \quad (34)$$

Here  $\mathbf{N}_1$  is the shape function matrix associated with element  $\Omega_1$  and is given by

$$\mathbf{N}_1 = \begin{bmatrix} \frac{x_1 - x}{L_1} & \frac{x - x_0}{L_1} \end{bmatrix}. \quad (35)$$

Following the Bubnov–Galerkin approach (see e.g. [30]), the virtual displacement is also assumed to vary linearly:

$$\delta \mathbf{u} = \mathbf{N}_1 \begin{Bmatrix} \delta \mathbf{u}_0 \\ \delta \mathbf{u}_1 \end{Bmatrix} \quad \text{in } \Omega_1. \quad (36)$$

Substituting (34) and (36) in (30), we obtain

$$\delta \mathbf{u}_0^T \mathbf{K} \mathbf{u}_0 \approx \begin{Bmatrix} \delta \mathbf{u}_0 \\ \delta \mathbf{u}_1 \end{Bmatrix}^T \bar{\mathbf{S}}_1 \begin{Bmatrix} \mathbf{u}_0 \\ \mathbf{u}_1 \end{Bmatrix} + \delta \mathbf{u}_1^T \mathbf{K} \mathbf{u}_1, \quad (37)$$

where  $\bar{\mathbf{S}}_1$  is the element stiffness matrix of  $\Omega_1$ :

$$\begin{aligned} \bar{\mathbf{S}}_1 &= \begin{bmatrix} \bar{\mathbf{S}}_1^{11} & \bar{\mathbf{S}}_1^{12} \\ \bar{\mathbf{S}}_1^{21} & \bar{\mathbf{S}}_1^{22} \end{bmatrix} = \int_{x=x_0}^{x=x_1} \left[ \frac{\partial \mathbf{N}^T}{\partial x} \mathbf{A} \frac{\partial \mathbf{N}}{\partial x} + \frac{\partial \mathbf{N}^T}{\partial x} \mathbf{B}_1 \mathbf{N} - \mathbf{N}^T \mathbf{B}_2 \frac{\partial \mathbf{N}}{\partial x} - \mathbf{N}^T \mathbf{D} \mathbf{N} \right] dx \\ &= \frac{1}{L_1} \begin{bmatrix} \mathbf{A} & -\mathbf{A} \\ -\mathbf{A} & \mathbf{A} \end{bmatrix} + \frac{1}{2} \begin{bmatrix} -\mathbf{B}_1 & -\mathbf{B}_1 \\ \mathbf{B}_1 & \mathbf{B}_1 \end{bmatrix} - \frac{1}{2} \begin{bmatrix} -\mathbf{B}_2 & \mathbf{B}_2 \\ -\mathbf{B}_2 & \mathbf{B}_2 \end{bmatrix} - \frac{L_1}{6} \begin{bmatrix} 2\mathbf{D} & \mathbf{D} \\ \mathbf{D} & 2\mathbf{D} \end{bmatrix}. \end{aligned} \quad (38)$$

The variational displacements can be eliminated in (37), resulting in the matrix form:

$$\begin{Bmatrix} \mathbf{K} \mathbf{u}_0 \\ 0 \end{Bmatrix} \approx \begin{bmatrix} \bar{\mathbf{S}}_1^{11} & \bar{\mathbf{S}}_1^{12} \\ \bar{\mathbf{S}}_1^{21} & \bar{\mathbf{S}}_1^{22} + \mathbf{K} \end{bmatrix} \begin{Bmatrix} \mathbf{u}_0 \\ \mathbf{u}_1 \end{Bmatrix} \quad \text{for any } \mathbf{u}_0. \quad (39)$$

It is important to note that the above relation is approximate, with errors resulting from finite-element discretization. The lack of exactness of (39) can be verified by examining a special case, where  $\mathbf{A}$ ,  $\mathbf{B}_1$ ,  $\mathbf{B}_2$ ,  $\mathbf{D}$  are scalar values (not operators). Then, (39) is exact if and only if

$$\mathbf{K}^2 = \bar{\mathbf{S}}_1^{11} \bar{\mathbf{S}}_1^{22} - \bar{\mathbf{S}}_1^{12} \bar{\mathbf{S}}_1^{21}. \quad (40)$$

We focus on the special case, where  $\mathbf{A} = 1$ ,  $\mathbf{B}_1 = \mathbf{B}_2 = 0$  and  $\mathbf{D} = 1$ , implying  $\bar{\mathbf{S}}_1^{11} = \bar{\mathbf{S}}_1^{22} = 1/L_1 - L_1/3$  and  $\bar{\mathbf{S}}_1^{12} = \bar{\mathbf{S}}_1^{21} = -1/L_1 - L_1/6$ . From (25), (23) and (32), we obtain the exact half-space stiffness  $\mathbf{K} = 1$ , which clearly does not satisfy (40), confirming the approximate nature of (39).

It turns out that a simple modification of the element stiffness matrix would eliminate the discretization errors in (39), and result in the *exact* half-space stiffness. This modification involves evaluating the integral in (38) using the mid-point rule (Fig. 1d), i.e. the expression for the element stiffness matrix is modified to

$$\mathbf{S}_1 = \frac{1}{L_1} \begin{bmatrix} \mathbf{A} & -\mathbf{A} \\ -\mathbf{A} & \mathbf{A} \end{bmatrix} + \frac{1}{2} \begin{bmatrix} -\mathbf{B}_1 & -\mathbf{B}_1 \\ \mathbf{B}_1 & \mathbf{B}_1 \end{bmatrix} - \frac{1}{2} \begin{bmatrix} -\mathbf{B}_2 & \mathbf{B}_2 \\ -\mathbf{B}_2 & \mathbf{B}_2 \end{bmatrix} - \frac{L_1}{4} \begin{bmatrix} \mathbf{D} & \mathbf{D} \\ \mathbf{D} & \mathbf{D} \end{bmatrix}. \tag{41}$$

With such a modification, which is the key to the proposed formulation, the error due to discretization and the error due to numerical integration cancel each other to result in the exact half-space stiffness (see Appendix A for the proof). It is important to note that  $\mathbf{S}_1$  is *not* the exact stiffness of the layer; but the half-space stiffness, obtained by replacing  $\bar{\mathbf{S}}_1$  by  $\mathbf{S}_1$  in (39), is *exact*, i.e.

$$\begin{Bmatrix} \mathbf{K}\mathbf{u}_0 \\ 0 \end{Bmatrix} = \begin{bmatrix} \mathbf{S}_1^{11} & \mathbf{S}_1^{12} \\ \mathbf{S}_1^{21} & \mathbf{S}_1^{22} + \mathbf{K} \end{bmatrix} \begin{Bmatrix} \mathbf{u}_0 \\ \mathbf{u}_1 \end{Bmatrix} \text{ for any } \mathbf{u}_0. \tag{42}$$

The above definition of the half-space stiffness can be recursively applied. The right half-space can be further split another finite element ( $\Omega_2 \equiv \{x_1 < x < x_2\}$ ) with mid-point integration and a half-space ( $x > x_2$ ). Applying this procedure infinite number of times, which is equivalent to discretizing the half-space into infinite number of finite elements as shown in Fig. 1e, would result in the (exact) discrete form of OWWE (after utilizing (33)):

$$\begin{Bmatrix} \mathbf{A} \partial \mathbf{u} / \partial x \\ 0 \\ 0 \\ \vdots \end{Bmatrix} + \begin{bmatrix} \mathbf{B}_1 + \mathbf{S}_1^{11} & \mathbf{S}_1^{12} & 0 & 0 \\ \mathbf{S}_1^{21} & \mathbf{S}_1^{22} + \mathbf{S}_2^{11} & \mathbf{S}_2^{12} & 0 \\ 0 & \mathbf{S}_2^{21} & \mathbf{S}_2^{22} + \mathbf{S}_3^{11} & \ddots \\ 0 & 0 & \ddots & \ddots \end{bmatrix} \begin{Bmatrix} \mathbf{u} \\ \mathbf{u}_1 \\ \mathbf{u}_2 \\ \vdots \end{Bmatrix} = \mathbf{0}, \tag{43}$$

where the expression for sub-matrices  $\mathbf{S}_j$  are defined in a way analogous to  $\mathbf{S}_1$  defined in (41) with the element length  $L_1$  replaced by  $L_j$ :

$$\mathbf{S}_j = \frac{1}{L_j} \begin{bmatrix} \mathbf{A} & -\mathbf{A} \\ -\mathbf{A} & \mathbf{A} \end{bmatrix} + \frac{1}{2} \begin{bmatrix} -\mathbf{B}_1 & -\mathbf{B}_1 \\ \mathbf{B}_1 & \mathbf{B}_1 \end{bmatrix} - \frac{1}{2} \begin{bmatrix} -\mathbf{B}_2 & \mathbf{B}_2 \\ -\mathbf{B}_2 & \mathbf{B}_2 \end{bmatrix} - \frac{L_j}{4} \begin{bmatrix} \mathbf{D} & \mathbf{D} \\ \mathbf{D} & \mathbf{D} \end{bmatrix}. \tag{44}$$

Note that, although we started with the analysis of a physical problem, the above can be considered as a mathematical identity with  $\mathbf{u}_j, j = 1, 2, 3, \dots$  being auxiliary variables, and  $L_j$  being the parameters of the expansion. We call this the *matrix continued-fraction form of OWWE* since the expansion is analogous to the matrix form of the scalar continued fraction expansion devised in [5]. Indeed, we can eliminate the auxiliary variables in (43) to obtain the formal expression:

$$-\left(\mathbf{A} \frac{\partial \mathbf{u}}{\partial x} + \mathbf{B}_1\right) = \mathbf{S}_1^{11} - \frac{\mathbf{S}_1^{12} \mathbf{S}_1^{21}}{\mathbf{S}_1^{22} + \mathbf{S}_2^{11} - \frac{\mathbf{S}_2^{12} \mathbf{S}_2^{21}}{\mathbf{S}_2^{22} + \mathbf{S}_3^{11} - \frac{\mathbf{S}_3^{12} \mathbf{S}_3^{21}}{\mathbf{S}_3^{22} + \mathbf{S}_4^{11} \dots}}}. \tag{45}$$

Note that the matrix continued fraction OWWE (43) is still exact, but is more tractable than the variational OWWE due to its discrete nature.

## 6. Arbitrarily wide-angle wave equations (AWWEs) using truncated continued-fraction expansions

The matrix continued-fraction OWWE derived in the previous section is still not suitable for computation due to the infinite number of auxiliary variables. In this section we make the OWWE computationally tractable by limiting the number of auxiliary variables, which is equivalent to mesh truncation. Such truncation introduces error, and the resulting OWWE is no longer exact. We study the approximation properties of the truncated continued fraction OWWE, and devise Arbitrarily Wide Angle Wave Equations (AWWEs) that are capable of representing waves traveling at an arbitrarily wide angle ( $-90^\circ < \theta < +90^\circ$ ) with the  $x$  axis.

The truncated continued-fraction OWWE is written as

$$\begin{Bmatrix} \mathbf{A} \partial \mathbf{u} / \partial x \\ \mathbf{0} \\ \vdots \\ \mathbf{0} \end{Bmatrix} + \begin{bmatrix} \mathbf{B}_1 + \mathbf{S}_1^{11} & \mathbf{S}_1^{12} & 0 & 0 \\ \mathbf{S}_1^{21} & \mathbf{S}_1^{22} + \mathbf{S}_2^{11} & \ddots & 0 \\ 0 & \ddots & \ddots & \mathbf{S}_{n-1}^{12} \\ 0 & 0 & \mathbf{S}_{n-1}^{21} & \mathbf{S}_{n-1}^{22} + \mathbf{S}_n^{11} \end{bmatrix} \begin{Bmatrix} \mathbf{u} \\ \mathbf{u}_1 \\ \vdots \\ \mathbf{u}_{n-1} \end{Bmatrix} = \mathbf{0}, \quad (46)$$

where only  $n - 1$  auxiliary variables are used. We call this the  $n$ -variable OWWE, considering the existence of a total of  $n$  variables. Physically speaking,  $n$ -variable OWWE is obtained by approximating the half-space stiffness by the stiffness of a truncated domain  $\{x_0 < x < x_n\}$  fixed on the right (Fig. 1f). It is immediately intuitive that the boundary condition on the right would result in reflections resulting in backward propagating waves that are as strong as forward propagating waves, indicating that the approximation in (46) is not sufficient for reasonably isolating forward propagating waves. This observation is made more precise by examining the approximation properties of the  $n$ -variable OWWE.

The principal approximation property can be summarized as follows (see Appendix B for the proof): the  $n$ -variable OWWE defined by (46) and (44) is exact for all the wave modes  $\mathbf{u} = \mathbf{a}e^{ikx}$  with

$$k = k_j = \frac{2i}{L_j}, \quad j = 1, \dots, n. \quad (47)$$

From this property, it follows that the proposed  $n$ -variable OWWE is exact for some evanescent modes (since  $k_j$  is imaginary), and approximates the dispersion relation by interpolating between these wavenumbers. It is natural to expect that as the number of auxiliary variables is increased, all the evanescent waves will be represented more accurately. On the other hand, irrespective of the number of auxiliary variables, the truncated continued fraction OWWE cannot properly represent the traveling waves, i.e. when the wavenumber is real.

The above problem can be resolved by noting again that the continued fraction OWWE is exact for  $k_j = 2i/L_j$ , where the parameters  $L_j$  can be chosen arbitrarily, i.e. they can be real, imaginary or even complex valued (the idea of choosing complex  $L_j$  is similar to the ideas of complex coordinate stretching used for unbounded domain analysis [31,32]). Equivalently, we can first choose wavenumbers  $k_j$  for which exact representation is desirable and accordingly fix  $L_j = 2i/k_j$ . By choosing  $k_j$  to be real (imaginary  $L_j$ ), propagating waves can be properly represented, while complex  $k_j$  (complex  $L_j$ ) would facilitate simultaneous representation of propagating as well as evanescent waves (see Fig. 1g). Furthermore, as will be shown in the next section, increasing the number of auxiliary variables will make the resulting truncated OWWE accurately represent waves propagating at wider range of angles. For this reason, we name the truncated  $n$ -variable OWWE with the flexibility of choosing complex  $k_j$ , the  $n$ -variable Arbitrarily Wide Angle Wave Equation (AWWE $_n$ ).

The final form of AWWE<sub>n</sub> is given by (46):

$$\begin{bmatrix} \mathbf{A}\partial/\partial x + \mathbf{B}_1 + \mathbf{S}_1^{11} & \mathbf{S}_1^{12} & 0 & 0 \\ \mathbf{S}_1^{21} & \mathbf{S}_1^{22} + \mathbf{S}_2^{11} & \ddots & 0 \\ 0 & \ddots & \ddots & \mathbf{S}_{n-1}^{12} \\ 0 & 0 & \mathbf{S}_{n-1}^{21} & \mathbf{S}_{n-1}^{22} + \mathbf{S}_n^{11} \end{bmatrix} \begin{Bmatrix} \mathbf{u} \\ \mathbf{u}_1 \\ \vdots \\ \mathbf{u}_{n-1} \end{Bmatrix} = \mathbf{0}, \tag{46}$$

where  $\mathbf{S}_j$  is defined as follows (obtained by substituting (47) in (44)):

$$\mathbf{S}_j = \frac{1}{2} \left( -ik_j \begin{bmatrix} \mathbf{A} & -\mathbf{A} \\ -\mathbf{A} & \mathbf{A} \end{bmatrix} + \begin{bmatrix} -\mathbf{B}_1 + \mathbf{B}_2 & -\mathbf{B}_1 - \mathbf{B}_2 \\ \mathbf{B}_1 + \mathbf{B}_2 & \mathbf{B}_1 - \mathbf{B}_2 \end{bmatrix} - \frac{i}{k_j} \begin{bmatrix} \mathbf{D} & \mathbf{D} \\ \mathbf{D} & \mathbf{D} \end{bmatrix} \right). \tag{48}$$

In the above,  $k_j$  are the parameters of AWWE, henceforth referred to as *reference wavenumbers*.

To summarize, the salient features of AWWE are:

- (a) AWWEs represent forward propagating waves associated with the general wave equations given by Eq. (19).
- (b) AWWE<sub>n</sub> is exact for waves with the horizontal wavenumber  $k = k_j, j = 1, \dots, n$ . Thus, knowledge of the approximate propagation characteristics could be used to design an effective AWWE.
- (c) AWWEs with real  $k_j$  represent only propagating waves. AWWEs with imaginary  $k_j$  represent only evanescent waves. AWWEs with complex  $k_j$ , or combination of real and imaginary  $k_j$ , can simultaneously represent propagating and evanescent waves.
- (d) As will be shown in the next section, increasing the number of auxiliary variables will make the AWWE accurate for wider range of angles. Also, for the same number of auxiliary variables, the overall accuracy of AWWE can be increased by the proper choice of the reference wavenumbers.
- (e) The above comment is restricted to the approximation properties of AWWEs. It is expected that special care must be administered in the choice of  $k_j$  in order to have an AWWE that is stable [22,23,26]. The notion of stability depends on the application; the stability for imaging problem may be different from stability for range-stepping problem, which in turn is different from the definition of stability in the context of absorbing boundaries. It is outside the scope of this paper to tackle these diverse stability issues. It should however be noted that AWWEs present themselves with the flexibility of choosing complex  $k_j$ , which is expected to be useful in obtaining stable versions for various applications [22,23,26].
- (f) AWWE derivation is based on choosing positive phase velocities. However, forward propagating waves have positive group velocity, but not necessarily positive phase velocity. In some cases involving anisotropic media or heterogeneous elastic media, there may be waves with positive group velocity, but negative phase velocity. It turns out that, for some special cases of anisotropy, AWWE is able to capture all the waves with positive group velocities including the ones with negative phase velocities. However, it is unclear at this time if AWWE can be successful in capturing all the forward propagating waves for more general cases. This open issue is currently under investigation and is outside the scope of this paper.

## 7. Applications

In this section, we specialize the general form of AWWE derived in the previous section to acoustics as well as to general anisotropic elasticity. The accuracy of the resulting AWWEs is examined with the help of slowness diagrams.

### 7.1. Scalar (acoustic) AWWE

By comparing (16) and (19), the coefficient “matrices” for the scalar wave equation are

$$\mathbf{A} = \mu, \quad \mathbf{B}_1 = \mathbf{B}_2 = 0, \quad \mathbf{D} = \rho\omega^2 + \frac{\partial}{\partial z} \left( \mu \frac{\partial}{\partial z} \right). \quad (49)$$

Referring to (48), the sub-matrices in AWWE are given by

$$\mathbf{S}_j = \frac{1}{2} \left( -ik_j \mu \begin{bmatrix} 1 & -1 \\ -1 & 1 \end{bmatrix} - \frac{i}{k_j} \left( \rho\omega^2 + \frac{\partial}{\partial z} \left( \mu \frac{\partial}{\partial z} \right) \right) \begin{bmatrix} 1 & 1 \\ 1 & 1 \end{bmatrix} \right). \quad (50)$$

Instead of choosing the reference wavenumbers, we choose *reference phase velocities* for which the AWWE is exact. Such a choice results in an AWWE that can be transformed easily into time domain. The reference wavenumbers are given by

$$k_j = \frac{\omega}{c_j}, \quad j = 1, \dots, n, \quad (51)$$

where  $c_j$  are the reference phase velocities. Substituting the above in (50), the sub-matrices take the form:

$$\mathbf{S}_j = \frac{-i\omega}{2} \begin{bmatrix} \mu/c_j + \rho c_j & -\mu/c_j + \rho c_j \\ -\mu/c_j + \rho c_j & \mu/c_j + \rho c_j \end{bmatrix} + \frac{\partial}{\partial z} \left( \frac{\mu}{2i\omega} \begin{bmatrix} c_j & c_j \\ c_j & c_j \end{bmatrix} \frac{\partial}{\partial z} \right). \quad (52)$$

Assembling the above sub-matrices into (46), we obtain the frequency-domain AWWE for acoustic waves:

$$\begin{Bmatrix} \mu \partial u / \partial x \\ 0 \\ \vdots \\ 0 \end{Bmatrix} - i\omega (\mu \mathbf{\Lambda}_1 + \rho \mathbf{\Lambda}_2) \begin{Bmatrix} u \\ u_1 \\ \vdots \\ u_{n-1} \end{Bmatrix} + \frac{1}{i\omega} \frac{\partial}{\partial z} \left( \mu \mathbf{\Lambda}_2 \frac{\partial}{\partial z} \begin{Bmatrix} u \\ u_1 \\ \vdots \\ u_{n-1} \end{Bmatrix} \right) = \mathbf{0}, \quad (53)$$

where

$$\mathbf{\Lambda}_1 = \frac{1}{2} \begin{bmatrix} 1/c_1 & -1/c_1 & 0 & 0 \\ -1/c_1 & 1/c_1 + 1/c_2 & \ddots & 0 \\ 0 & \ddots & \ddots & -1/c_{n-1} \\ 0 & 0 & -1/c_{n-1} & (1/c_{n-1} + 1/c_n) \end{bmatrix}, \quad (54)$$

$$\mathbf{\Lambda}_2 = \frac{1}{2} \begin{bmatrix} c_1 & c_1 & 0 & 0 \\ c_1 & c_1 + c_2 & \ddots & 0 \\ 0 & \ddots & \ddots & c_{n-1} \\ 0 & 0 & c_{n-1} & c_{n-1} + c_n \end{bmatrix}. \quad (55)$$

The time-domain acoustic AWWE is obtained by taking inverse Fourier transform of the frequency-domain AWWE:

$$\begin{pmatrix} \mu \partial^2 u / \partial x \partial t \\ 0 \\ \vdots \\ 0 \end{pmatrix} + (\mu \Lambda_1 + \rho \Lambda_2) \frac{\partial^2}{\partial t^2} \begin{pmatrix} u \\ u_1 \\ \vdots \\ u_{n-1} \end{pmatrix} - \frac{\partial}{\partial z} \left( \mu \Lambda_2 \frac{\partial}{\partial z} \begin{pmatrix} u \\ u_1 \\ \vdots \\ u_{n-1} \end{pmatrix} \right) = \mathbf{0}. \tag{56}$$

It is easy to show that the above equation is identical to the OWWEs derived based on conventional continued fraction expansion in the context of absorbing boundaries [5]. It is shown in [5] that the OWWEs derived in that paper are generalizations of the approximations proposed by Engquist and Majda [4]. In fact it can be shown that acoustic AWWEs, with all the reference phase velocities chosen as a single value, are identical to the OWWEs proposed by Engquist and Majda. It should be noted that acoustic AWWEs can be shown to be equivalent to the OWWEs proposed by Bamberger et al. [12], but are different in their form, indicating that the implementation aspects are different [33,34] from the implementation of Bamberger’s OWWEs [14]. An implementation of acoustic AWWE in time-space domain can be found in [35], where AWWE has been utilized for seismic migration.

The accuracy of acoustic AWWEs is examined using the dispersion relations for homogeneous free space and comparing with the (exact) dispersion relationship obtained from the full wave equation. The dispersion relationship for the full wave equation, written in terms of the horizontal slowness  $\bar{k} = k/\omega$  and vertical slowness  $\bar{l} = l/\omega$ , is given by

$$\bar{k}^2 + \bar{l}^2 = \frac{1}{c^2}, \tag{57}$$

where  $c = \sqrt{\mu/\rho}$  is the wave velocity. The exact dispersion relationship for OWWE representing forward propagating waves is obtained by taking the positive root of the horizontal slowness  $\bar{k}$ :

$$\bar{k} = \sqrt{\frac{1}{c^2} - \bar{l}^2}. \tag{58}$$

It is convenient to represent the dispersion relationship in terms of the slowness diagram [28], which is the plot of the relation in the slowness  $(\bar{k}, \bar{l})$  space. It follows that the exact slowness diagram takes the form of a semicircle/hyperbola as shown in Fig. 2. Note that only half of the diagram associated with positive vertical slowness is shown.

The approximate dispersion relationship associated with AWWE is obtained by first writing AWWE in terms of  $\bar{k}, \bar{l}$ . By Fourier transforming the frequency-domain AWWE in space and rearranging, we obtain

$$\begin{pmatrix} \bar{k}u \\ 0 \\ \vdots \\ 0 \end{pmatrix} - \left( \Lambda_1 + \left( \frac{1}{c^2} - \bar{l}^2 \right) \Lambda_2 \right) \begin{pmatrix} u \\ u_1 \\ \vdots \\ u_{n-1} \end{pmatrix} = \mathbf{0}. \tag{59}$$

The auxiliary variables  $u_1, \dots, u_{n-1}$  can be eliminated to obtain an equation of the form:

$$[\bar{k} - F_n(\bar{l})]u = 0, \tag{60}$$

resulting in the dispersion relation  $\bar{k} = F_n(\bar{l})$ , which can be plotted as a slowness diagram.

The slowness diagrams for several acoustic AWWEs are compared with the exact slowness diagram in Figs. 2–5. For the sake of presentation, the wave velocity is chosen as  $c = 1$ . Fig. 2 shows the slowness diagram for AWWE<sub>1</sub> with  $c_1 = c$ . It can be clearly observed that the slowness is exact for  $\bar{k} = \bar{k}_1 = 1/c = 1$ , while the remaining slowness diagram is approximated. Increasing the number of variables increases the accuracy; the slowness associated with AWWE<sub>3</sub> with  $c_1 = c_2 = c_3 = c$  (Fig. 3) is clearly more accurate than

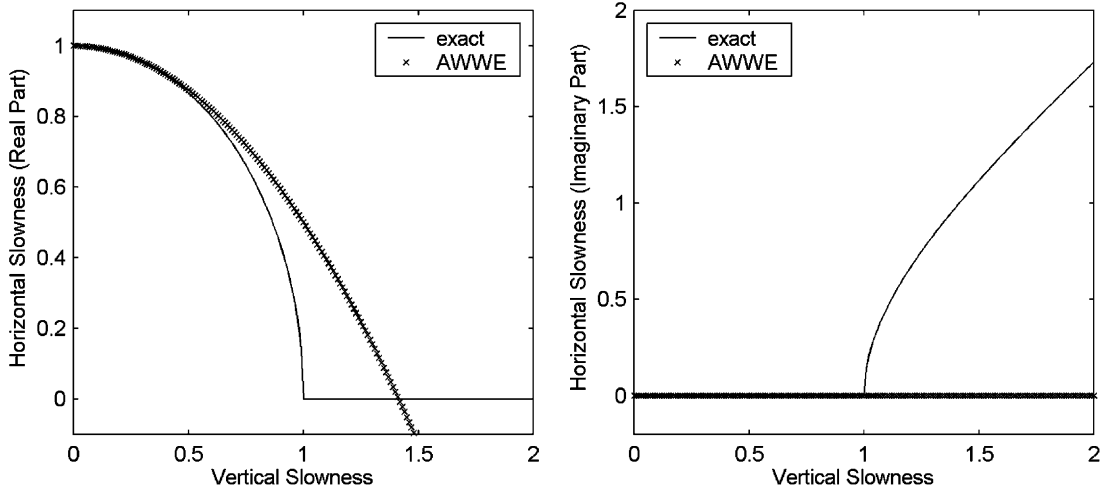


Fig. 2. Slowness diagram for acoustic AWWE<sub>1</sub> with  $c_1 = c$ .

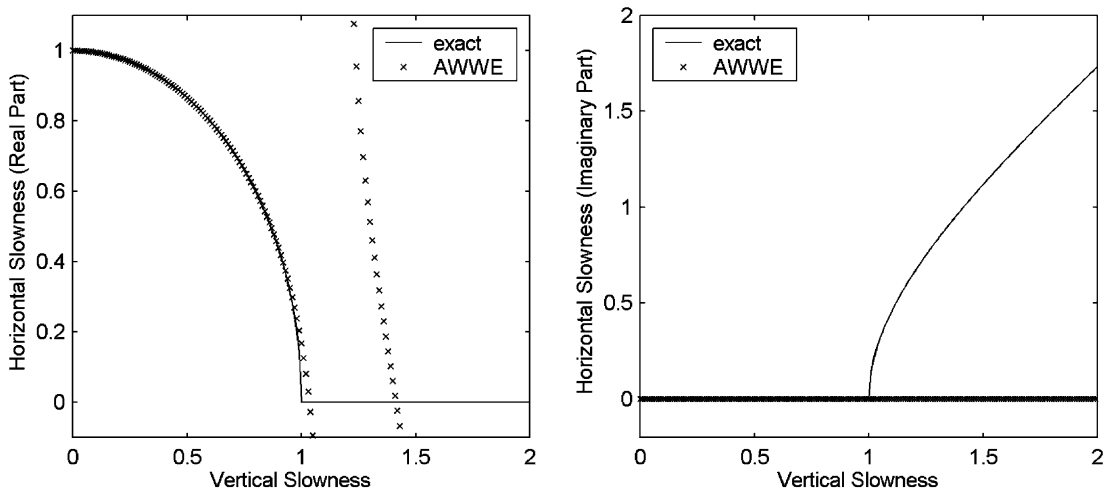


Fig. 3. Slowness diagram for acoustic AWWE<sub>3</sub> with  $c_1 = c_2 = c_3 = c$ .

that of AWWE<sub>1</sub> in Fig. 2. Fig. 4 shows the slowness diagram for AWWE<sub>2</sub> with  $c_1 = c, c_2 = 4c$ . By comparing Figs. 3 and 4, it can be clearly seen that AWWE<sub>2</sub> with  $c_1 = c, c_2 = 4c$  is more accurate than AWWE<sub>3</sub> with  $c_1 = c_2 = c_3 = c$ , illustrating that the flexibility provided by AWWE in choosing the reference wavenumbers can aid in further increasing its accuracy.

It is clear from Figs. 2–4 that real  $c_j$  would always result in a real horizontal slowness, thus completely misrepresenting evanescent waves. If evanescent waves are also to be represented (e.g. in some problems of unbounded domain modeling), complex  $c_j$  can be used. Fig. 5 contains the slowness diagram of AWWE<sub>5</sub> with  $c_j = nc/((1 + i)^j)$ . Both real and imaginary branches of the slowness match well with the exact slowness, illustrating the effectiveness of AWWE in modeling propagating as well as evanescent waves.

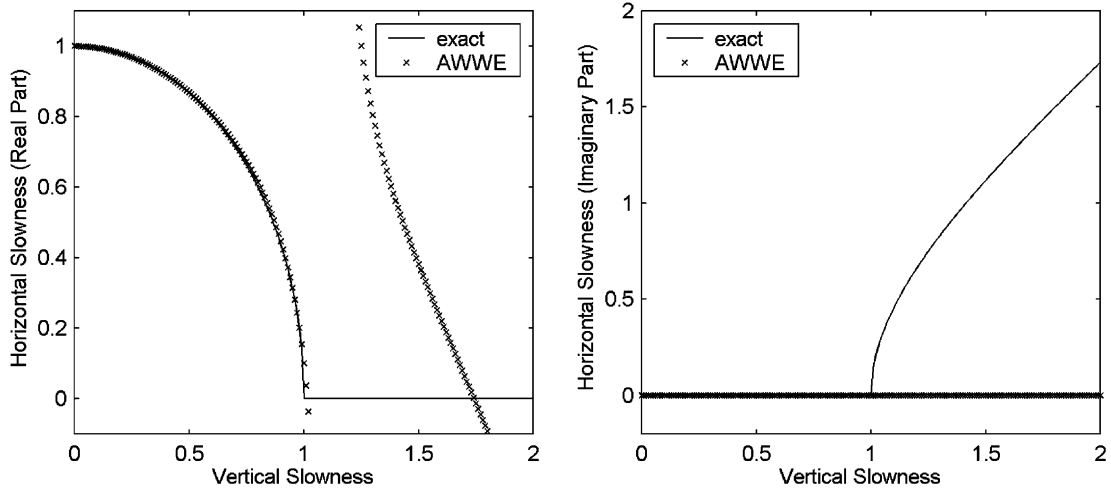


Fig. 4. Slowness diagram for acoustic AWWE<sub>2</sub> with  $c_1 = c$ ,  $c_2 = 4c$ .

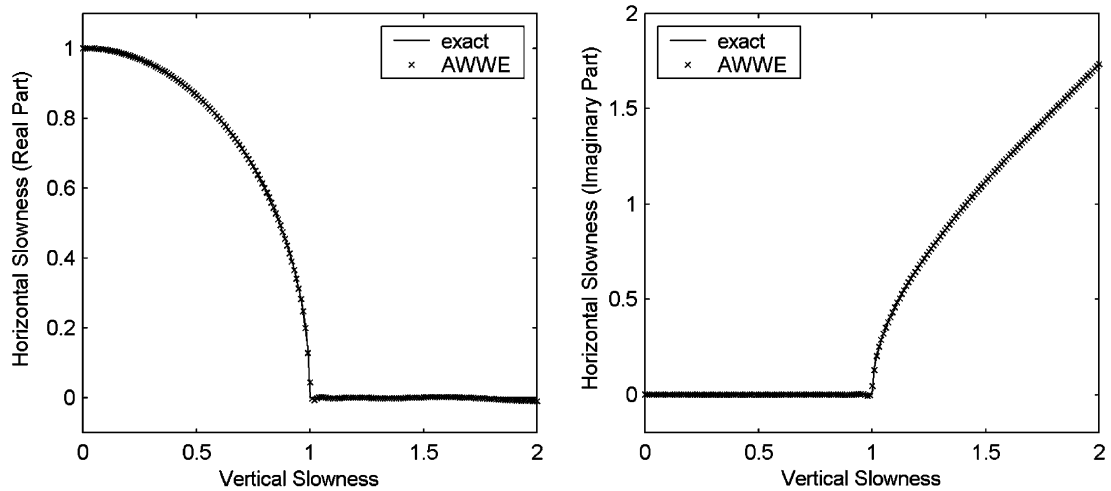


Fig. 5. Slowness diagram for acoustic AWWE<sub>5</sub> with  $c_j = nc/(1 + ij)$ .

### 7.2. Elastic AWWE

This section contains the derivation of AWWE for general anisotropic elastic media, while the accuracy properties of the resulting AWWE are examined in the following two sections. Comparing the elastic wave equation (5) and the model equation (19), we note that

$$\mathbf{A} = \mathbf{G}_{xx}, \quad \mathbf{B}_1 = \mathbf{G}_{xz} \frac{\partial}{\partial z}, \quad \mathbf{C} = \frac{\partial}{\partial z} \mathbf{G}_{xz}^T, \quad \mathbf{D} = \mathbf{M}\omega^2 + \frac{\partial}{\partial z} \mathbf{G}_{zz} \frac{\partial}{\partial z}. \quad (61)$$

Similar to the acoustic AWWE, the reference phase velocities  $c_j$  are chosen first, indicating that the reference wavenumbers are given by

$$k_j = \frac{\omega}{c_j}, \quad j = 1, \dots, n. \quad (62)$$

The sub-matrices in AWWE are obtained by substituting (61), (62) in (48):

$$\begin{aligned} \mathbf{S}_j = & -i\omega \left( \frac{1}{2c_j} \begin{bmatrix} \mathbf{G}_{xx} & -\mathbf{G}_{xx} \\ -\mathbf{G}_{xx} & \mathbf{G}_{xx} \end{bmatrix} + \frac{c_j}{2} \begin{bmatrix} \mathbf{M} & \mathbf{M} \\ \mathbf{M} & \mathbf{M} \end{bmatrix} \right) + \frac{1}{2} \begin{bmatrix} -\mathbf{G}_{xz} & -\mathbf{G}_{xz} \\ \mathbf{G}_{xz} & \mathbf{G}_{xz} \end{bmatrix} \frac{\partial}{\partial z} \\ & + \frac{1}{2} \frac{\partial}{\partial z} \begin{bmatrix} \mathbf{G}_{xz}^T & -\mathbf{G}_{xz}^T \\ \mathbf{G}_{xz}^T & -\mathbf{G}_{xz}^T \end{bmatrix} - \frac{ic_j}{2\omega} \frac{\partial}{\partial z} \begin{bmatrix} \mathbf{G}_{zz} & \mathbf{G}_{zz} \\ \mathbf{G}_{zz} & \mathbf{G}_{zz} \end{bmatrix} \frac{\partial}{\partial z}. \end{aligned} \quad (63)$$

Substituting the above expression in (46) would result in the frequency-domain elastic AWWE<sub>n</sub>:

$$\begin{aligned} & \begin{Bmatrix} \mathbf{G}_{xx} \frac{\partial \mathbf{u}}{\partial x} \\ \mathbf{0} \\ \vdots \\ \mathbf{0} \end{Bmatrix} - i\omega(\Lambda_1 + \Lambda_2) \begin{Bmatrix} \mathbf{u} \\ \mathbf{u}_1 \\ \vdots \\ \mathbf{u}_{n-1} \end{Bmatrix} + \Lambda_3 \frac{\partial}{\partial z} \begin{Bmatrix} \mathbf{u} \\ \mathbf{u}_1 \\ \vdots \\ \mathbf{u}_{n-1} \end{Bmatrix} + \frac{\partial}{\partial z} \left( \bar{\Lambda}_3 \begin{Bmatrix} \mathbf{u} \\ \mathbf{u}_1 \\ \vdots \\ \mathbf{u}_{n-1} \end{Bmatrix} \right) \\ & + \frac{1}{i\omega} \frac{\partial}{\partial z} \left( \Lambda_4 \frac{\partial}{\partial z} \begin{Bmatrix} \mathbf{u} \\ \mathbf{u}_1 \\ \vdots \\ \mathbf{u}_{n-1} \end{Bmatrix} \right) = \mathbf{0}, \end{aligned} \quad (64)$$

where

$$\Lambda_1 = \frac{1}{2} \begin{bmatrix} \frac{1}{c_1} \mathbf{G}_{xx} & -\frac{1}{c_1} \mathbf{G}_{xx} & \mathbf{0} & \mathbf{0} \\ -\frac{1}{c_1} \mathbf{G}_{xx} & \left( \frac{1}{c_1} + \frac{1}{c_2} \right) \mathbf{G}_{xx} & \ddots & \mathbf{0} \\ \mathbf{0} & \ddots & \ddots & -\frac{1}{c_{n-1}} \mathbf{G}_{xx} \\ \mathbf{0} & \mathbf{0} & -\frac{1}{c_{n-1}} \mathbf{G}_{xx} & \left( \frac{1}{c_{n-1}} + \frac{1}{c_n} \right) \mathbf{G}_{xx} \end{bmatrix}, \quad (65)$$

$$\Lambda_2 = \frac{1}{2} \begin{bmatrix} c_1 \mathbf{M} & c_1 \mathbf{M} & \mathbf{0} & \mathbf{0} \\ c_1 \mathbf{M} & (c_1 + c_2) \mathbf{M} & \ddots & \mathbf{0} \\ \mathbf{0} & \ddots & \ddots & c_{n-1} \mathbf{M} \\ \mathbf{0} & \mathbf{0} & c_{n-1} \mathbf{M} & (c_{n-1} + c_n) \mathbf{M} \end{bmatrix}, \quad (66)$$

$$\Lambda_3 = \frac{1}{2} \begin{bmatrix} \mathbf{G}_{xz} & -\mathbf{G}_{xz} & \mathbf{0} & \mathbf{0} \\ \mathbf{G}_{xz} & \mathbf{0} & \ddots & \mathbf{0} \\ \mathbf{0} & \ddots & \ddots & -\mathbf{G}_{xz} \\ \mathbf{0} & \mathbf{0} & \mathbf{G}_{xz} & \mathbf{0} \end{bmatrix}, \quad (67)$$

$$\bar{\Lambda}_3 = \frac{1}{2} \begin{bmatrix} \mathbf{G}_{xz}^T & -\mathbf{G}_{xz}^T & \mathbf{0} & \mathbf{0} \\ \mathbf{G}_{xz}^T & \mathbf{0} & \ddots & \mathbf{0} \\ \mathbf{0} & \ddots & \ddots & -\mathbf{G}_{xz}^T \\ \mathbf{0} & \mathbf{0} & \mathbf{G}_{xz}^T & \mathbf{0} \end{bmatrix}, \quad (68)$$

$$\Lambda_4 = \frac{1}{2} \begin{bmatrix} c_1 \mathbf{G}_{zz} & c_1 \mathbf{G}_{zz} & \mathbf{0} & \mathbf{0} \\ c_1 \mathbf{G}_{zz} & (c_1 + c_2) \mathbf{G}_{zz} & \ddots & \mathbf{0} \\ \mathbf{0} & \ddots & \ddots & c_{n-1} \mathbf{G}_{zz} \\ \mathbf{0} & \mathbf{0} & c_{n-1} \mathbf{G}_{zz} & (c_{n-1} + c_n) \mathbf{G}_{zz} \end{bmatrix}. \tag{69}$$

The time-domain form of the elastic AWWE is obtained by taking the inverse Fourier transform of (64) and is given by

$$\begin{aligned} & \left\{ \begin{matrix} \mathbf{G}_{xx} \frac{\partial^2 \mathbf{u}}{\partial x \partial t} \\ \mathbf{0} \\ \vdots \\ \mathbf{0} \end{matrix} \right\} + (\Lambda_1 + \Lambda_2) \frac{\partial^2}{\partial t^2} \left\{ \begin{matrix} \mathbf{u} \\ \mathbf{u}_1 \\ \vdots \\ \mathbf{u}_{n-1} \end{matrix} \right\} + \Lambda_3 \frac{\partial^2}{\partial z \partial t} \left\{ \begin{matrix} \mathbf{u} \\ \mathbf{u}_1 \\ \vdots \\ \mathbf{u}_{n-1} \end{matrix} \right\} \\ & + \frac{\partial}{\partial z} \left( \Lambda_3 \frac{\partial}{\partial t} \left\{ \begin{matrix} \mathbf{u} \\ \mathbf{u}_1 \\ \vdots \\ \mathbf{u}_{n-1} \end{matrix} \right\} \right) - \frac{\partial}{\partial z} \left( \Lambda_4 \frac{\partial}{\partial z} \left\{ \begin{matrix} \mathbf{u} \\ \mathbf{u}_1 \\ \vdots \\ \mathbf{u}_{n-1} \end{matrix} \right\} \right) = \mathbf{0}. \end{aligned} \tag{70}$$

We reemphasize here that the elastic AWWE given in the previous paragraph is applicable for general anisotropic media. This is in contrast to other elastic OWWEs, which are limited to either isotropic elasticity or transversely isotropic elasticity with material symmetry about the coordinate axes. Furthermore, unlike the existing elastic OWWEs, elastic AWWEs are completely in terms of displacements. It is thus possible to use the elastic AWWEs not only for range stepping problems, but also for downward continuation in the context of three-component seismic imaging, and for modeling unbounded domains in the context of wave propagation modeling. Another property of elastic AWWEs is that they are self-adjoint in terms of  $z$ , making them attractive for numerical implementation. Finally, the form of AWWEs is very similar to the 15° acoustic wave equation (except for the third and fourth terms which do not add any complications), indicating that the implementation can be derived from numerical schemes designed for 15° acoustic OWWE.

### 7.3. Accuracy of AWWE for isotropic elasticity

Similar to the acoustic AWWEs, the accuracy of elastic AWWEs is verified by examining the dispersion relationship for the special case of homogeneous isotropic media. The exact dispersion relationship, obtained from the full wave equation, is given by

$$\bar{k}_p = \sqrt{\frac{1}{c_p^2} - \bar{l}^2} \quad \text{and} \quad \bar{k}_s = \sqrt{\frac{1}{c_s^2} - \bar{l}^2}, \tag{71}$$

where  $\bar{l}$  is the vertical wavenumber,  $\bar{k}_p$  and  $\bar{k}_s$  are horizontal wavenumbers associated with pressure and shear waves respectively.  $c_p$  and  $c_s$  are the pressure and shear wave velocities and are given by

$$c_p = \sqrt{\frac{\lambda + 2\mu}{\rho}} \quad \text{and} \quad c_s = \sqrt{\frac{\mu}{\rho}}. \tag{72}$$

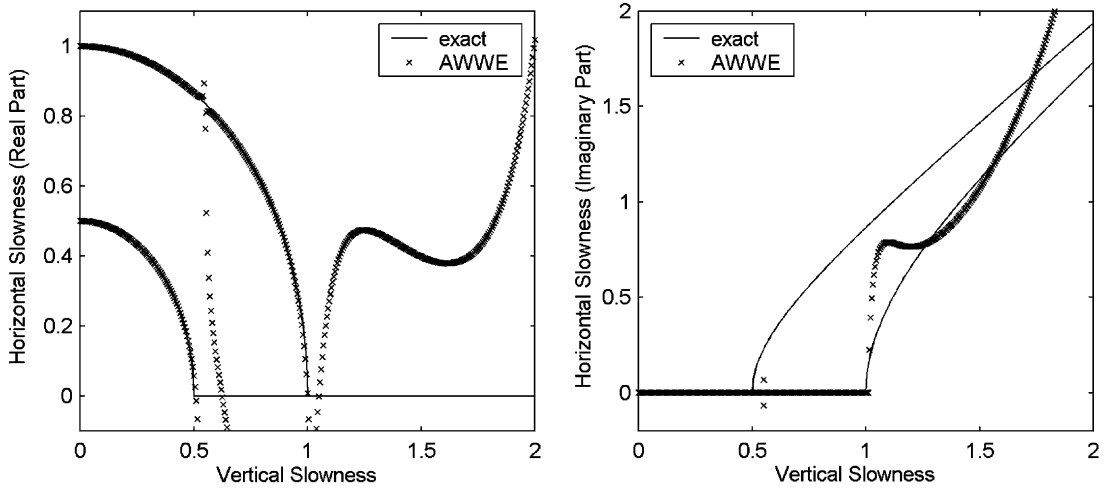


Fig. 6. Slowness diagram for elastic AWWE<sub>3</sub> with  $c_j = nc_s/j$ .

The exact slowness diagrams are given by two concentric semi-circles and associated hyperbolae as shown in Fig. 6; again, only half of the slowness diagram associated with positive vertical slowness is shown in the figure.

The approximate dispersion relationship is obtained by Fourier transforming the frequency-domain AWWE (64) in space, and writing AWWE in terms of normalized wavenumbers  $\bar{k}$  and  $\bar{l}$ :

$$\begin{Bmatrix} \bar{k}\mathbf{G}_{xx}\mathbf{u} \\ \mathbf{0} \\ \vdots \\ \mathbf{0} \end{Bmatrix} + \left( -(\Lambda_1 + \Lambda_2) + \bar{l}(\Lambda_3 + \bar{\Lambda}_3) + \bar{l}^2\Lambda_4 \right) \begin{Bmatrix} \mathbf{u} \\ \mathbf{u}_1 \\ \vdots \\ \mathbf{u}_{n-1} \end{Bmatrix} = \mathbf{0}. \tag{73}$$

The auxiliary variables  $\mathbf{u}_1, \dots, \mathbf{u}_{n-1}$  can be eliminated to obtain an equation of the form

$$(\bar{k}\mathbf{G}_{xx} - \mathbf{F}_n(\bar{l}))\mathbf{u} = \mathbf{0}, \tag{74}$$

indicating that the normalized horizontal wavenumbers are the eigenvalues of  $\mathbf{F}_n$  with respect to  $\mathbf{G}_{xx}$ .

The slowness diagrams for several AWWEs are compared with the exact slowness diagram in Figs. 6 and 7. For the sake of presentation, the Poisson’s ratio is chosen as 1/3 with the wave velocities  $c_s = 1$  and  $c_p = 2$ . Fig. 6 shows the slowness diagrams of AWWE<sub>3</sub> with the reference phase velocities chosen as  $c_j = nc_s/j$ . With such a choice of  $c_j$ , AWWE<sub>3</sub> happens to be highly accurate for all propagating (pressure and shear) waves. In order to simultaneously represent propagating and evanescent waves, a series of AWWEs are obtained using complex reference velocities  $c_j = nc_p/((1 + 1.5i)j)$ . The slowness resulting from AWWE<sub>3</sub> is not very accurate (not shown here), and it was necessary to increase the order to 7. Fig. 7 shows the slowness diagrams of AWWE<sub>7</sub>, which are almost exact for propagating waves as well as evanescent waves associated with the range shown in the figure.

#### 7.4. Accuracy of AWWE for anisotropic elasticity

In this section, the accuracy of AWWE is examined for several cases of anisotropic media: (a) transversely isotropic (TI) media with a principal material axis coinciding with the  $x$  axis; and (b) tilted trans-

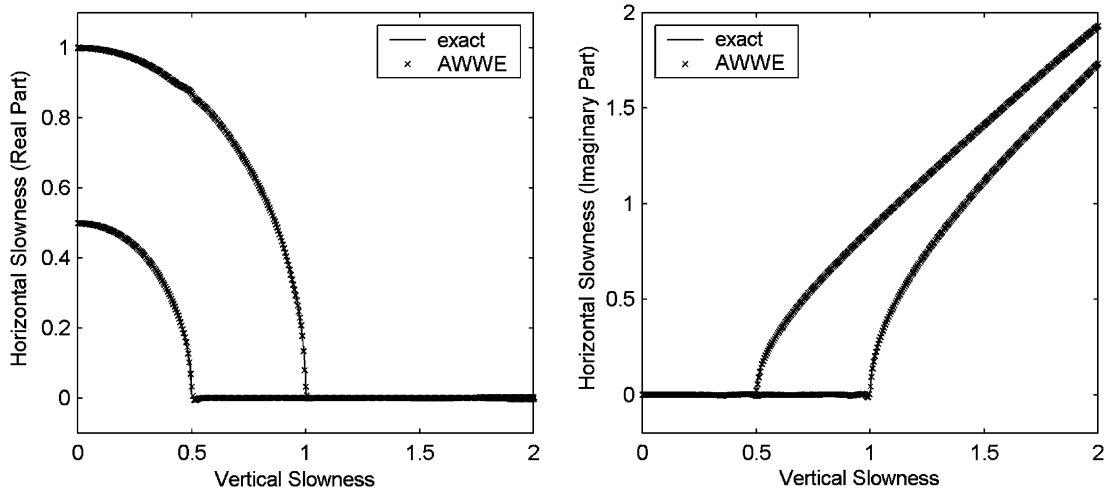


Fig. 7. Slowness diagram for elastic AWWE<sub>7</sub> with  $c_j = nc_s/(1 + 1.5i)$ .

versely isotropic (TTI) media with a principal material axis not coinciding with the  $x$  axis. Thomsen’s representation of TI media [36] is adopted here. Essentially, the elements of the elasticity matrix are given by (derived from [36])

$$\begin{aligned}
 E_{22} &= \rho c_p^2, \\
 E_{33} &= \rho c_s^2, \\
 E_{11} &= (1 + 2\varepsilon)E_{22}, \\
 E_{12} = E_{21} &= \sqrt{((1 + 2\delta)E_{22} - E_{33})(E_{22} - E_{33})} - E_{33}, \\
 E_{13} = E_{31} = E_{23} = E_{32} &= 0,
 \end{aligned} \tag{75}$$

where  $\varepsilon$  and  $\delta$  are the parameters of anisotropy, and  $c_p$  and  $c_s$  are respectively pressure and shear wave velocities. If the two parameters of anisotropy are equal, the exact slowness diagrams are elliptical (elliptic anisotropy). If they are different, the slowness diagrams tend to be more complex (non-elliptic anisotropy). For TTI media, the elasticity matrix in (75) is transformed from the principal material directions to the coordinate axes with the help of tensor transformation.

Here, we examine the performance of AWWE for elliptic and non-elliptic, TI and TTI media. The slowness diagrams for these cases are generated in a manner identical to that for isotropic elasticity. Due to the complex nature of the slowness diagrams, and to facilitate effective discussion of one-way propagation in anisotropic media, the slowness diagram for the AWWE is presented in conjunction with the complete slowness diagram of the two-way wave equation.

**Case 1 (TI with elliptic anisotropy).** A TI material with strong elliptic anisotropy is considered. The anisotropy parameters are  $\varepsilon = 0.6$  and  $\delta = 0.6$ , while for most rocks they are smaller than 0.4 [36]. Fig. 8 shows the slowness diagram of AWWE<sub>8</sub> with  $c_j = nc_s/(1 + i)$ , clearly illustrating that the forward propagating waves are accurately captured.

**Case 2 (TTI with elliptic anisotropy).** The TI media considered in Case 1 is tilted in this example by 45°, resulting in the rotation of the slowness diagram. The main difference between this example and the examples discussed till now is that this case contains modes for which the group velocity (the vector normal to the real part of the slowness curve) is in the positive  $x$  direction, while the phase velocity (the vector

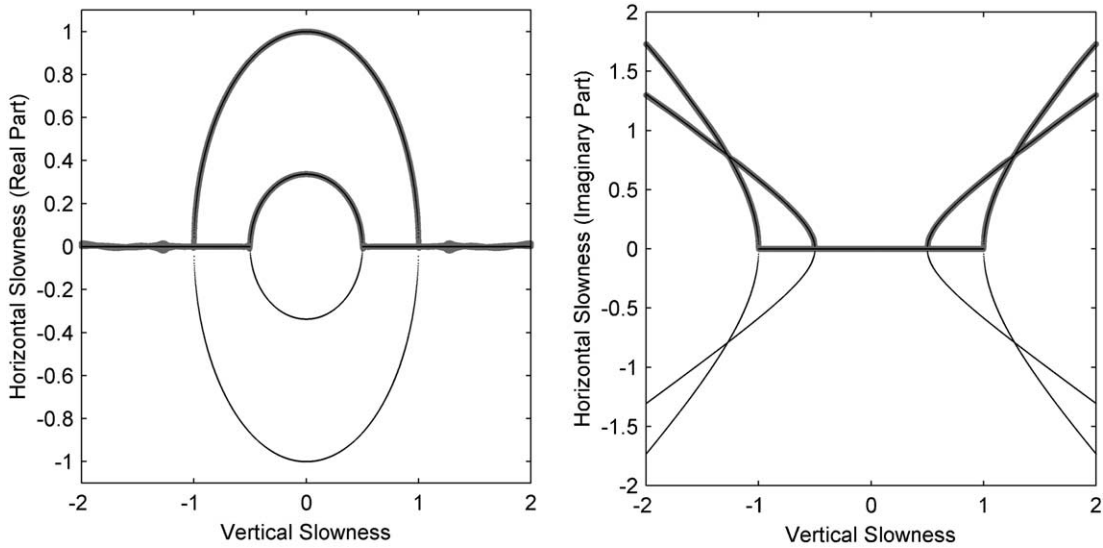


Fig. 8. Slowness diagram for elastic AWE<sub>8</sub> with  $c_j = nc_s/(1 + i)$ . The thick gray lines are the slowness of AWE, while the thin solid lines represent the slowness of the full wave equation. Note that some parts of the solid lines are masked by the gray lines.

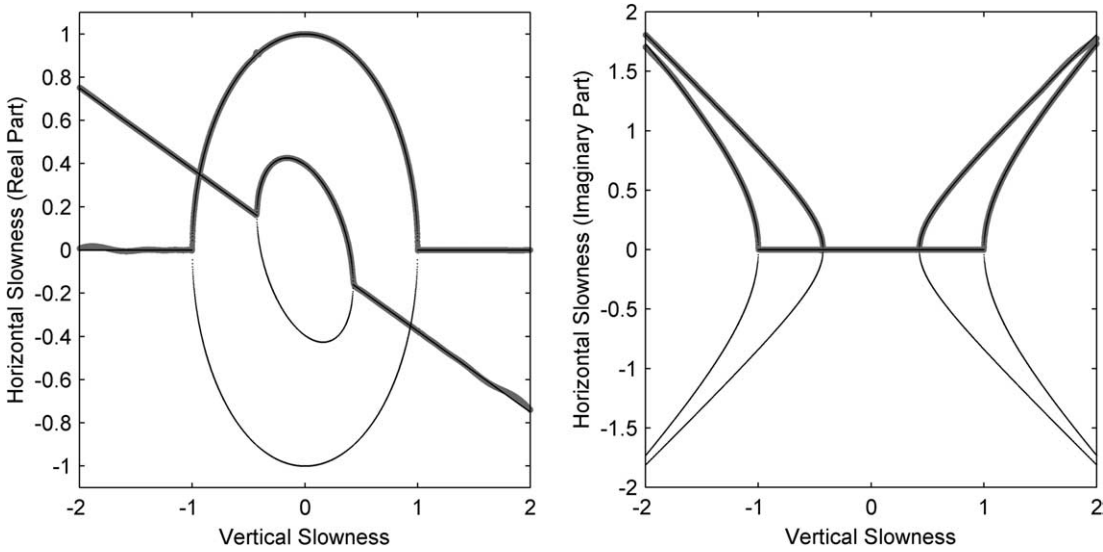


Fig. 9. Slowness diagram for elastic AWE<sub>9</sub> with  $c_j = nc_s/(1 + i)$ . The thick gray lines are the slowness of AWE, while the thin solid lines represent the slowness of the full wave equation. Note that some parts of the solid lines are masked by the gray lines.

connecting the origin to a point on the slowness curve) is in the negative  $x$  direction. To be precise, OWWEs need to be derived based on group velocities (energy propagation velocities) and not based on the phase velocities. However, AWE formulation is based on phase velocities and it is not clear if it would work for this particular case. Surprisingly, AWE seems to capture all the waves with positive group velocities (not phase velocities; see Fig. 9). At this time, it is unclear how AWE is able to capture this branch; further analysis will be conducted in the future.

**Case 3 (TI with non-elliptic anisotropy).** In this case, the anisotropy parameters are changed to  $\varepsilon = 0.2$  and  $\delta = -0.2$ , making the slowness diagram non-elliptic. The resulting slowness (see Fig. 10) is less complex than the previous case in that the positive-group-velocity branches coincide with the positive-phase-velocity branches. Nevertheless, the slowness is non-elliptic and is more complex than in Case 1. As expected, despite the complex shape of slowness diagram, AWWE captures the correct branch of the slowness.

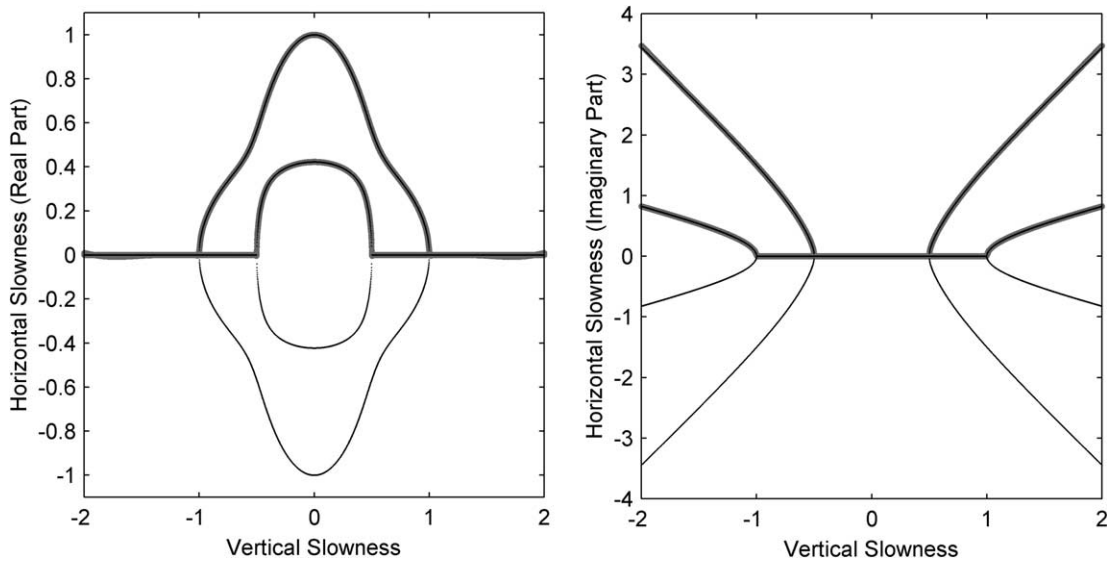


Fig. 10. Slowness diagram for elastic AWWE<sub>9</sub> with  $c_j = nc_s((1 + i)j)$ . The thick gray lines are the slowness of AWWE, while the thin solid lines represent the slowness of the full wave equation. Note that some parts of the solid lines are masked by the gray lines.

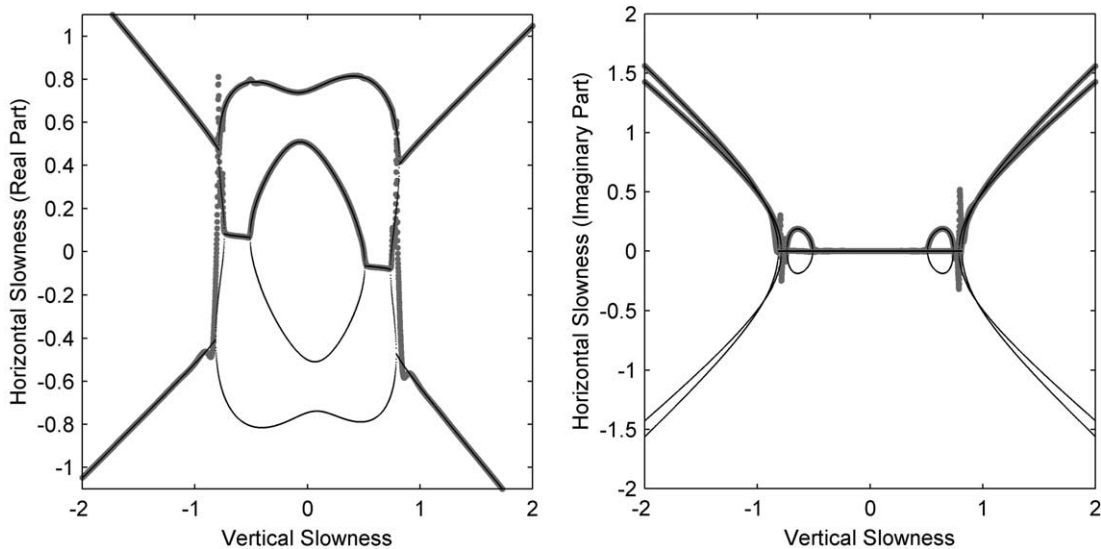


Fig. 11. Slowness diagram for elastic AWWE<sub>10</sub> with  $c_j = nc_s((1 + 2i)j)$ . The thick gray lines are the slowness of AWWE, while the thin solid lines represent the slowness of the full wave equation. Note that some parts of the solid lines are masked by the gray lines.

**Case 4 (TTI with non-elliptic anisotropy).** The TI media of the previous case is tilted by  $45^\circ$ , making the slowness even more complex, i.e. the slowness is not elliptic, and in addition, the positive-group-velocity branches do not match with the positive-phase-velocity branches. Unfortunately, for this case, AWWE is unable to capture the correct branch of the diagram (see Fig. 11). This is in contrast with the AWWE's success in capturing the correct branch in elliptic TTI media. At this time, it is unclear as to when and how the correct branch is captured by AWWE. It may be possible for AWWE to capture the correct branch if the parameters are chosen properly. This possibility is currently under investigation and will be reported in a future publication if successful.

## 8. Summary and conclusions

In this paper, we developed a systematic procedure for deriving arbitrarily wide-angle wave equations (AWWEs), which are highly accurate and computationally tractable time–space and frequency–space representations of one-way propagation of waves in complex range-independent heterogeneous, anisotropic viscoelastic porous media. AWWEs are derived using a seven-step procedure (see Fig. 1): (a) representing one-way wave equations in terms of half-space stiffness relations; (b) writing the half-space stiffness in a recursive variational form by splitting the half-space into a layer and another half-space; (c) approximating the variational form by replacing the layer with a finite element; (d) eliminating the approximation through one-point integration resulting in an exact discrete recursive form; (e) recursively applying the discrete form to represent half-space stiffness with infinite number of finite elements with one-point integration—at the end, this results in a matrix continued fraction expansion of the one-way propagator; (f) truncating the number of elements to make it computationally tractable, which is equivalent to truncated continued fraction approximation of the operator; and (g) using imaginary finite-element lengths to represent traveling waves, or complex lengths to represent both traveling and evanescent waves.

AWWEs have several desirable properties. They are simple in their form and are similar to the well-known  $15^\circ$  acoustic OWWE. The only difference is that AWWEs involve auxiliary variables. AWWEs are arbitrarily accurate with their accuracy increased by simply increasing the number of auxiliary variables. AWWEs are transparent in their representation; they exactly propagate waves with their wavelengths coinciding with the reference wavelengths, which are the parameters of the AWWE. The flexibility offered by AWWEs in representing evanescent waves (using imaginary and complex reference wavenumbers) is expected to aid in obtaining stable elastic AWWEs for various applications [26]. Most importantly, AWWEs appear to have the capability of representing one-way propagation in any media where the full wave equation is a second order differential equation in space.

While the derivation procedure is applicable for general second order hyperbolic systems, the accuracy of AWWE depends on the parameters of AWWE. In this paper, the parameters are chosen in an ad-hoc manner. Such a choice of the parameters works well for deriving accurate AWWE for acoustic and isotropic elastic waves, as well as some special cases of anisotropic elasticity. The preliminary versions of AWWE for more general anisotropy appear to have difficulty in capturing the correct branch of the slowness diagram. It may be possible to obtain the correct branch of slowness through more appropriate choice of the AWWE parameters, but this possibility is not explored here and is a subject of future study.

The AWWEs developed in this paper have several practical applications: (a) the heterogeneous acoustic AWWE has already been successfully applied to imaging [35] and unbounded domain analysis [37,38] (b) the isotropic elastic AWWE, due to its displacement-based form, appears to be the first higher order space-domain OWWE that has immediate applicability to subsurface imaging and unbounded domain modeling; moreover, (c) AWWE for elliptically anisotropic media derived in this paper appears to be the first high order OWWE for tilted transversely isotropic (TTI) media.

In spite of the above contributions, the study reported in this paper should be considered preliminary, with several unresolved issues that are subjects of ongoing and future studies. They are: (a) a more systematic procedure for choosing the AWE parameters for optimal accuracy; (b) AWE for general anisotropy (careful study of the effect of AWE parameters is needed for exploring the possibility of capturing the correct branch of the slowness diagram); (c) AWE for arbitrarily heterogeneous media (the current development is limited to range-independent heterogeneity and it would be desirable to obtain AWE where the material properties vary with the preferred direction, i.e. range-dependent media); (d) use of AWE for various applications (the current development focuses on the theoretical accuracy of the equation). When it comes to solving AWE for various application problems, stability as well as numerical implementation play an important role. These aspects are not considered in this paper due to their problem-dependent nature. Applications of acoustic AWE are reported in separate publications [35,37,38], while more complex applications of elastic AWE are currently under investigation.

### Acknowledgments

This material is based upon work supported by the National Science Foundation under Grant No. CMS-0100188. Any opinions, findings, and conclusions or recommendations expressed in this material are those of the authors and do not necessarily reflect the views of the National Science Foundation. The author wishes to thank Professor John L. Tassoulas of the University of Texas at Austin for suggesting several improvements in the paper, and Professor Kerry Havner and Homayoun Heidari for their careful review of the manuscript.

### Appendix A. Proof of the exactness of the half-space stiffness relation

Here, we verify the exactness of the half-space stiffness relation, i.e.

$$\begin{Bmatrix} \mathbf{K}\mathbf{u}_0 \\ 0 \end{Bmatrix} \stackrel{?}{=} \begin{bmatrix} \mathbf{S}_1^{11} & \mathbf{S}_1^{12} \\ \mathbf{S}_1^{21} & \mathbf{S}_1^{22} + \mathbf{K} \end{bmatrix} \begin{Bmatrix} \mathbf{u}_0 \\ \mathbf{u}_1 \end{Bmatrix} \quad \text{for any } \mathbf{u}_0, \quad (76)$$

or equivalently,

$$\begin{bmatrix} \mathbf{S}_1^{11} - \mathbf{K} & \mathbf{S}_1^{12} \\ \mathbf{S}_1^{21} & \mathbf{S}_1^{22} + \mathbf{K} \end{bmatrix} \begin{Bmatrix} \mathbf{u}_0 \\ \mathbf{u}_1 \end{Bmatrix} \stackrel{?}{=} \begin{Bmatrix} \mathbf{0} \\ \mathbf{0} \end{Bmatrix} \quad \text{for any } \mathbf{u}_0. \quad (77)$$

Since  $\mathbf{u}_1$  is an auxiliary variable dependent on  $\mathbf{u}_0$ , it is sufficient to prove that, for any  $\mathbf{u}_0$ , there exists a  $\mathbf{u}_1$  such that (77) is true.

We prove the above claim for a wave mode of the form  $\mathbf{u} = \mathbf{a}e^{ikx}$ , with arbitrarily chosen horizontal wavenumber  $k$ . Naturally,  $\mathbf{a}$ , and thus  $\mathbf{u}_0$ , satisfy the dispersion relation (21). Furthermore, since the traction  $\mathbf{F}_0 = (\mathbf{A}\partial\mathbf{u}/\partial x + \mathbf{B}_1\mathbf{u})|_{x=0}$ , the exact half-space stiffness relation can be written as

$$\mathbf{K}\mathbf{u}_0 = -(ik\mathbf{A} + \mathbf{B}_1)\mathbf{u}_0. \quad (78)$$

In what follows, we show that  $\mathbf{u}_1$  also satisfies the exact stiffness relation, i.e.

$$\mathbf{K}\mathbf{u}_1 = -(ik\mathbf{A} + \mathbf{B}_1)\mathbf{u}_1. \quad (79)$$

It follows that, since exact half-space stiffness relation is conceptually a factorized version of the full dispersion relationship (21),  $\mathbf{u}_1$  satisfies (21).

The above claims ((77) and (79)) can be rewritten as: for any  $\mathbf{u}_0$  satisfying (78), there exists a  $\mathbf{u}_1$  satisfying (79) such that (77) is true. For the remainder of the proof, we replace  $\mathbf{u}_0$  and  $\mathbf{u}_1$  with  $\mathbf{a}_0$  and  $\mathbf{a}_1$  respectively, to emphasize the focus on wave modes.

Substituting (41), (78) and (79) in (77), it is sufficient to verify that

$$\left( \begin{array}{c} \frac{1}{L_1} \begin{bmatrix} \mathbf{A} & -\mathbf{A} \\ -\mathbf{A} & \mathbf{A} \end{bmatrix} + \frac{1}{2} \begin{bmatrix} -\mathbf{B}_1 & -\mathbf{B}_1 \\ \mathbf{B}_1 & \mathbf{B}_1 \end{bmatrix} - \frac{1}{2} \begin{bmatrix} -\mathbf{B}_2 & \mathbf{B}_2 \\ -\mathbf{B}_2 & \mathbf{B}_2 \end{bmatrix} \\ -\frac{L_1}{4} \begin{bmatrix} \mathbf{D} & \mathbf{D} \\ \mathbf{D} & \mathbf{D} \end{bmatrix} + \begin{bmatrix} ik\mathbf{A} + \mathbf{B}_1 & 0 \\ 0 & -ik\mathbf{A} - \mathbf{B}_1 \end{bmatrix} \end{array} \right) \begin{Bmatrix} \mathbf{a}_0 \\ \mathbf{a}_1 \end{Bmatrix} \stackrel{?}{=} \begin{Bmatrix} \mathbf{0} \\ \mathbf{0} \end{Bmatrix} \quad \text{for any } \mathbf{a}_0. \quad (80)$$

Using (21), we note that

$$(\mathbf{B}_1 + \mathbf{B}_2)\mathbf{a}_0 = -\left[ ik\mathbf{A} + \frac{\mathbf{D}}{ik} \right] \mathbf{a}_0 \quad \text{and} \quad (\mathbf{B}_1 + \mathbf{B}_2)\mathbf{a}_1 = -\left[ ik\mathbf{A} + \frac{\mathbf{D}}{ik} \right] \mathbf{a}_1. \quad (81)$$

Substituting the above equations in (80) results in

$$\left[ \begin{array}{cc} \left( \frac{1}{L_1} + \frac{ik}{2} \right) \mathbf{A} - \left( \frac{L_1}{4} + \frac{1}{2ik} \right) \mathbf{D} & \left( -\frac{1}{L_1} + \frac{ik}{2} \right) \mathbf{A} - \left( \frac{L_1}{4} - \frac{1}{2ik} \right) \mathbf{D} \\ \left( -\frac{1}{L_1} - \frac{ik}{2} \right) \mathbf{A} - \left( \frac{L_1}{4} + \frac{1}{2ik} \right) \mathbf{D} & \left( \frac{1}{L_1} - \frac{ik}{2} \right) \mathbf{A} - \left( \frac{L_1}{4} - \frac{1}{2ik} \right) \mathbf{D} \end{array} \right] \begin{Bmatrix} \mathbf{a}_0 \\ \mathbf{a}_1 \end{Bmatrix} \stackrel{?}{=} \begin{Bmatrix} \mathbf{0} \\ \mathbf{0} \end{Bmatrix} \quad \text{for any } \mathbf{a}_0. \quad (82)$$

Multiplying both sides by the nonsingular matrix  $\begin{bmatrix} +L_1/2 & -L_1/2 \\ -ik & -ik \end{bmatrix}$ , it is sufficient to verify that

$$\left[ \begin{array}{cc} \left( 1 + \frac{ikL_1}{2} \right) \mathbf{A} & \left( -1 + \frac{ikL_1}{2} \right) \mathbf{A} \\ \left( 1 + \frac{ikL_1}{2} \right) \mathbf{D} & \left( -1 + \frac{ikL_1}{2} \right) \mathbf{D} \end{array} \right] \begin{Bmatrix} \mathbf{a}_0 \\ \mathbf{a}_1 \end{Bmatrix} \stackrel{?}{=} \begin{Bmatrix} \mathbf{0} \\ \mathbf{0} \end{Bmatrix} \quad \text{for any } \mathbf{a}_0. \quad (83)$$

The above equality can be readily verified by choosing

$$\mathbf{a}_1 = \left( \frac{1 + ikL_1/2}{1 - ikL_1/2} \right) \mathbf{a}_0. \quad (84)$$

Thus, we have shown that the stiffness expansion given in (42) is exact when mid-point integration rule is used.

**Remark.** Note that  $\mathbf{a}_1$  can be viewed as the wave mode  $\mathbf{a}_0$  propagated through the finite element layer from  $x = 0$  to  $x = L_1$ . It is clear from (84) that  $\mathbf{a}_1$  is parallel to  $\mathbf{a}_0$ , indicating that the shape of the wave mode is not altered by propagation. However, it is important to recognize that the propagation is only approximate. Since  $\mathbf{u} = \mathbf{a}_0 e^{ikx}$ , the exact expression for the propagated mode is  $\mathbf{a}_1 = \mathbf{u}|_{x=L_1} = e^{ikL_1} \mathbf{a}_0$ , which is different from (84). It can be easily seen that the expression in the parentheses in (84) is an approximation of  $e^{ikL_1}$ . This approximation is completely erroneous for large values of  $L_1$ , indicating that, in general, no physical significance should be attached to the variables  $\mathbf{a}_1, \mathbf{a}_2, \dots$ . These auxiliary variables, however, do satisfy the exact dispersion relationship, a property that is useful in the proof of the AWWE's principal approximation property given in Appendix B.

## Appendix B. Proof of the approximation property of the $n$ -variable OWWE

The principal approximation property is that the  $n$ -variable OWWE given in (46) is exact for all the wave modes with wavenumber equal to  $2i/L_j, j = 1, \dots, n$ , i.e.

$$\begin{Bmatrix} ik\mathbf{A}\mathbf{a} \\ \mathbf{0} \\ \vdots \\ \mathbf{0} \end{Bmatrix} + \begin{bmatrix} \mathbf{B}_1 + \mathbf{S}_1^{11} & \mathbf{S}_1^{12} & 0 & 0 \\ \mathbf{S}_1^{21} & \mathbf{S}_1^{22} + \mathbf{S}_2^{11} & \ddots & 0 \\ 0 & \ddots & \ddots & \mathbf{S}_{n-1}^{12} \\ 0 & 0 & \mathbf{S}_{n-1}^{21} & \mathbf{S}_{n-1}^{22} + \mathbf{S}_n^{11} \end{bmatrix} \begin{Bmatrix} \mathbf{a} \\ \mathbf{a}_1 \\ \vdots \\ \mathbf{a}_{n-1} \end{Bmatrix} = \mathbf{0} \quad \begin{array}{l} \text{for any } \mathbf{a}, \\ \text{for } k = k_j = \frac{2i}{L_j}. \end{array} \quad (85)$$

In order to prove the above property, we first prove that the domain  $\{x_{j-1} < x < x_n\}$  fixed at the right results in the exact half-space stiffness for the wave mode with wavenumber  $k_j$ , i.e.

$$\begin{Bmatrix} ik_j\mathbf{A}\mathbf{a}_{j-1} \\ \mathbf{0} \\ \vdots \\ \mathbf{0} \end{Bmatrix} + \begin{bmatrix} \mathbf{B}_1 + \mathbf{S}_j^{11} & \mathbf{S}_j^{12} & 0 & 0 \\ \mathbf{S}_j^{21} & \mathbf{S}_j^{22} + \mathbf{S}_j^{11} & \ddots & 0 \\ 0 & \ddots & \ddots & \mathbf{S}_{n-1}^{12} \\ 0 & 0 & \mathbf{S}_{n-1}^{21} & \mathbf{S}_{n-1}^{22} + \mathbf{S}_n^{11} \end{bmatrix} \begin{Bmatrix} \mathbf{a}_{j-1} \\ \mathbf{a}_j \\ \vdots \\ \mathbf{a}_{n-1} \end{Bmatrix} \stackrel{?}{=} \mathbf{0} \quad \text{for any } \mathbf{a}_{j-1}. \quad (86)$$

Note that  $L_j = 2i/k_j$ ,  $\mathbf{S}_j$  can be evaluated from (44) as

$$\mathbf{S}_j = \frac{k_j}{2i} \begin{bmatrix} \mathbf{A} & -\mathbf{A} \\ -\mathbf{A} & \mathbf{A} \end{bmatrix} + \frac{1}{2} \begin{bmatrix} -\mathbf{B}_1 + \mathbf{B}_2 & -\mathbf{B}_1 - \mathbf{B}_2 \\ \mathbf{B}_1 + \mathbf{B}_2 & \mathbf{B}_1 - \mathbf{B}_2 \end{bmatrix} - \frac{i}{2k_j} \begin{bmatrix} \mathbf{D} & \mathbf{D} \\ \mathbf{D} & \mathbf{D} \end{bmatrix}, \quad (87)$$

which can be rearranged as

$$\begin{aligned} \mathbf{S}_j &= \frac{1}{2ik_j} \left( k_j^2 \begin{bmatrix} \mathbf{A} & -\mathbf{A} \\ -\mathbf{A} & \mathbf{A} \end{bmatrix} + ik_j \begin{bmatrix} -\mathbf{B}_1 + \mathbf{B}_2 & -\mathbf{B}_1 - \mathbf{B}_2 \\ \mathbf{B}_1 + \mathbf{B}_2 & \mathbf{B}_1 - \mathbf{B}_2 \end{bmatrix} + \begin{bmatrix} \mathbf{D} & \mathbf{D} \\ \mathbf{D} & \mathbf{D} \end{bmatrix} \right) \\ &= \frac{1}{2ik_j} \begin{bmatrix} \mathbf{A}k_j^2 - ik_j\mathbf{B}_1 + ik_j\mathbf{B}_2 + \mathbf{D} & -\mathbf{A}k_j^2 - ik_j\mathbf{B}_1 - ik_j\mathbf{B}_2 + \mathbf{D} \\ -\mathbf{A}k_j^2 + ik_j\mathbf{B}_1 + ik_j\mathbf{B}_2 + \mathbf{D} & \mathbf{A}k_j^2 + ik_j\mathbf{B}_1 - ik_j\mathbf{B}_2 + \mathbf{D} \end{bmatrix}. \end{aligned} \quad (88)$$

Substituting the above expression into (85), we obtain

$$\begin{aligned} &\frac{1}{2ik_j} \begin{bmatrix} -\mathbf{A}k_j^2 + ik_j\mathbf{B}_1 + ik_j\mathbf{B}_2 + \mathbf{D} & -\mathbf{A}k_j^2 - ik_j\mathbf{B}_1 - ik_j\mathbf{B}_2 + \mathbf{D} & \mathbf{0} & \mathbf{0} \\ -\mathbf{A}k_j^2 + ik_j\mathbf{B}_1 + ik_j\mathbf{B}_2 + \mathbf{D} & \mathbf{A}k_j^2 + ik_j\mathbf{B}_1 - ik_j\mathbf{B}_2 + \mathbf{D} + \mathbf{S}_j^{11} & \ddots & \mathbf{0} \\ \mathbf{0} & \ddots & \ddots & \mathbf{S}_{n-1}^{12} \\ \mathbf{0} & \mathbf{0} & \mathbf{S}_{n-1}^{21} & \mathbf{S}_{n-1}^{22} + \mathbf{S}_n^{11} \end{bmatrix} \\ &\times \begin{Bmatrix} \mathbf{a}_{j-1} \\ \mathbf{a}_j \\ \vdots \\ \mathbf{a}_{n-1} \end{Bmatrix} \stackrel{?}{=} \mathbf{0} \quad \text{for any } \mathbf{a}_{j-1}. \end{aligned} \quad (89)$$

Noting that  $\mathbf{a}_{j-1}$  satisfies the dispersion relation of the full wave equation, the above equation translates into

$$\begin{bmatrix} \mathbf{0} & -\mathbf{A}k_j^2 - ik_j\mathbf{B}_1 - ik_j\mathbf{B}_2 + \mathbf{D} & \mathbf{0} & \mathbf{0} \\ \mathbf{0} & \mathbf{A}k_j^2 + ik_j\mathbf{B}_1 - ik_j\mathbf{B}_2 + \mathbf{D} + \mathbf{S}_j^{11} & \ddots & \mathbf{0} \\ \mathbf{0} & \ddots & \ddots & \mathbf{S}_{n-1}^{12} \\ \mathbf{0} & \mathbf{0} & \mathbf{S}_{n-1}^{21} & \mathbf{S}_{n-1}^{22} + \mathbf{S}_n^{11} \end{bmatrix} \begin{Bmatrix} \mathbf{a}_{j-1} \\ \mathbf{a}_j \\ \vdots \\ \mathbf{a}_{n-1} \end{Bmatrix} \stackrel{?}{=} \mathbf{0} \quad \text{for any } \mathbf{a}_{j-1}. \quad (90)$$

It is straightforward to verify the above equation by simply eliminating the variables  $\mathbf{a}_j$  to  $\mathbf{a}_{n-1}$ . It is thus shown that the domain  $\{x_{j-1} < x < x_n\}$  exactly represents the half-space stiffness for wave modes with wavenumber  $k_j$ . It then follows from the recursive definition of  $\mathbf{K}$  in (42) that the domain  $\{x_{j-2} < x < x_n\}$  and eventually  $\{x_0 < x < x_n\}$  represent the exact half-space stiffness for the specific wave mode. We thus conclude that the  $n$ -variable OWWE is exact for wave modes with  $k_j = 2i/L_j$  for  $j = 1, \dots, n$ .

## References

- [1] J.F. Claerbout, *Imaging the Earth's Interior*, Blackwell Scientific Publications, 1985.
- [2] Y.-F. Chang, C. Chir-Cherng, Frequency-wavenumber migration of ultrasonic data, *J. Nondestructive Evaluat.* 19 (2000) 1–10.
- [3] D. Lee, A.D. Pierce, E.C. Shang, Parabolic equation development in the twentieth century, *J. Comput. Acoust.* 8 (2000) 527–637.
- [4] B. Engquist, A. Majda, Radiation boundary conditions for acoustic and elastic wave calculations, *Commun. Pure Appl. Math.* 32 (1979) 313–357.
- [5] M.N. Guddati, J.L. Tassoulas, Continued-fraction absorbing boundary conditions for the wave equation, *J. Comput. Acoust.* 8 (2000) 139–156.
- [6] J. Gazdag, Wave equation migration with phase-shift method, *Geophysics* 43 (1978) 1342–1351.
- [7] K.J. Langenberg, M. Brandfab, R. Hannemann, T. Kaczorowski, J. Kostka, C. Hofmann, R. Marklein, K. Mayer, A. Pitsch, Inverse scattering with acoustic, electromagnetic, and elastic waves as applied in nondestructive evaluation, in: A. Wirgin (Ed.), *Wavefield Inversion*, vol. 398, CISM Courses and Lectures, Springer Wein, 1999, pp. 59–118.
- [8] P.L. Stoffa, J.T. Fokkema, R.M. de Luna Freire, W.P. Kessinger, Split-step Fourier migration, *Geophysics* 55 (1990) 410–421.
- [9] D. Ristow, T. Ruhl, Fourier finite-difference migration, *Geophysics* 59 (1994) 1882–1893.
- [10] R.S. Wu, Wide-angle elastic-wave one-way propagation in heterogeneous media and an elastic-wave complex-screen method, *J. Geophys. Res. Solid Earth* 99 (1994) 751–766.
- [11] E.L. Lindman, “Free-space” boundary conditions for the time-dependent wave equation, *J. Comput. Phys.* 18 (1975) 66–78.
- [12] A. Bamberger, B. Engquist, L. Halpern, P. Joly, Higher-order paraxial wave-equation approximations in heterogeneous media, *SIAM J. Appl. Math.* 48 (1988) 129–154.
- [13] A. Bamberger, B. Engquist, L. Halpern, P. Joly, Parabolic wave-equation approximations in heterogeneous media, *SIAM J. Appl. Math.* 48 (1988) 99–128.
- [14] M.D. Collins, Applications and time-domain solution of higher-order parabolic equations in underwater acoustics, *J. Acoust. Soc. Am.* 86 (1989) 1097–1102.
- [15] D. Givoli, High-order local non-reflecting boundary conditions: a review, *Wave Motion* 39 (2004) 319–326.
- [16] T. Landers, J.F. Claerbout, Numerical calculations of elastic waves in laterally heterogeneous media, *J. Geophys. Res.* 77 (1972) 1476–1483.
- [17] J.J. McCoy, Parabolic theory of stress wave-propagation through inhomogeneous linearly elastic solids, *J. Appl. Mech.* 44 (1977) 462–468.
- [18] S.C. Wales, J.J. McCoy, A comparison of parabolic wave theories for linearly elastic solids, *Wave Motion* 5 (1983) 99–113.
- [19] J.A. Hudson, A parabolic approximation for elastic-waves, *Wave Motion* 2 (1980) 207–214.
- [20] J. Coronas, B. Defacio, R.J. Krueger, Parabolic approximations to the time-independent elastic wave-equation, *J. Math. Phys.* 23 (1982) 577–586.
- [21] R.R. Greene, A high-angle one-way wave-equation for seismic wave propagation along rough and sloping interfaces, *J. Acoust. Soc. Am.* 77 (1985) 1991–1998.
- [22] B.T.R. Wetton, G.H. Brooke, One-way wave-equations for seismoacoustic propagation in elastic wave-guides, *J. Acoust. Soc. Am.* 87 (1990) 624–632.

- [23] M.D. Collins, Higher-order Pade approximations for accurate and stable elastic parabolic equations with application to interface wave-propagation, *J. Acoust. Soc. Am.* 89 (1991) 1050–1057.
- [24] A.J. Fredricks, W.L. Siegmman, M.D. Collins, A parabolic equation for anisotropic elastic media, *Wave Motion* 31 (2000) 139–146.
- [25] M.D. Collins, W.A. Kuperman, W.L. Siegmman, A parabolic equation for poro-elastic media, *J. Acoust. Soc. Am.* 98 (1995) 1645–1656.
- [26] F.A. Milinazzo, C.A. Zala, G.H. Brooke, Rational square-root approximations for parabolic equation algorithms, *J. Acoust. Soc. Am.* 101 (1997) 760–766.
- [27] P.M. Morse, K.U. Ingard, *Theoretical Acoustics*, Princeton University Press, Princeton, 1986.
- [28] J.D. Achenbach, *Wave Propagation in Elastic Solids*, North-Holland, Amsterdam, 1973.
- [29] M.A. Biot, Theory of propagation of elastic waves in fluid-saturated porous solid—I: low-frequency range, *J. Acoust. Soc. Am.* 29 (1956) 168–178.
- [30] E.B. Becker, G.F. Carey, J.T. Oden, *Finite Elements—An Introduction*, vol. 1, Prentice-Hall, Englewood Cliffs, NJ, 1981.
- [31] W.C. Chew, J. Jin, E. Michielssen, Complex coordinate stretching as a generalized absorbing boundary condition, *Microwave Opt. Technol. Lett.* 15 (1997) 363–369.
- [32] S. Asvadurov, V. Druskin, M.N. Guddati, L. Knizhnerman, On optimal finite-difference approximation of PML, *SIAM J. Numer. Anal.* 41 (2003) 287–305.
- [33] M.N. Guddati, A.H. Heidari, Application of arbitrarily-wide angle wave equations for subsurface imaging and nondestructive evaluation, in: EM2003, 16th ASCE Engineering Mechanics Conference, Seattle, 2003.
- [34] A.H. Heidari, M.N. Guddati, Migration with arbitrarily wide-angle wave equations, in: 73rd Annual Meeting of the Society of Exploration Geophysicists, Dallas, TX, 2003.
- [35] M.N. Guddati, A.H. Heidari, Migration with arbitrarily wide-angle wave equations, *Geophysics*, to appear.
- [36] L. Thomsen, Weak anisotropic elasticity, *Geophysics* 51 (1986) 1954–1966.
- [37] K.-W. Lim, Absorbing boundary conditions for corner regions, M.S. Thesis, Civil Engineering, North Carolina State University, Raleigh, 2003, p. 92.
- [38] M.N. Guddati, K.-W. Lim, Continued fraction absorbing boundary conditions for convex polygonal domains, *Int. J. Numer. Methods Engrg.*, in revision.